Supplementary Material (ESI) for CrystEngComm

Structures and conformational analysis of a 3 × 3 isomer grid of nine *N*-(fluorophenyl)pyridinecarboxamides

Pavle Mocilac,[a] Alan J. Lough[b] John F. Gallagher*[a]

Targeted Therapeutics and Theranostics (T^3) Programme

[a] *School of Chemical Sciences, Dublin City University, Dublin 9, Ireland*
[b] *Department of Chemistry, University of Toronto, 80 St. George Street, Toronto, Ontario, Canada M5S 3H6*

Electronic Supplementary Information

Table of Contents

1. Detailed description of synthetic procedures

As acyl chlorides are very reactive, the reactions were performed in anhydrous conditions in CH_2Cl_2 (under N_2), initially at 5°C and then at room temperature. A by-product is HCl, and triethylamine (Et_3N) was employed to drive the reaction equilibrium towards the **NxxF** product. The pyridinoyl chlorides technically were used in the form of hydrochlorides so an additional mole of Et_3N was used to enhance their solubility in CH_2Cl_2 so that in total, two molar equivalents of triethylamine (Et_3N) were added.

Condensation reactions were performed with the 4-, 3- or 2-fluoroanilines (1 ml, 10.41 mmol) added to a 250 ml flask placed on an ice bath and with subsequent stirring. Then, 30 ml of CH_2Cl_2 was added to the flask followed by addition of Et_3N (1.5 ml, 10.76 mmol). Finally, the 4-, 3- or 2-pyridinoyl chlorides (2 g, 11.23 mmol) were added in portions directly into this solution mixture. Another 30 ml of CH_2Cl_2 and 1.5 ml of NEt_3 was added to accelerate the dissolution of any solids and the reaction mixture was allowed to warm to room temperature and stirred overnight.

Organic washing and work-up was as standard: the organic reaction phase was washed with 20 ml of $KHCO_3$ (0.1 M) solution *ca*. 3-7 times and during purification, glassware was warmed to *ca*. 35°C. Then, 1.5 g of anhydrous $MgSO_4$ was added to the organic solutions for 20 minutes. The flask contents were filtered through a Büchner funnel (under vacuum) to remove $MgSO_4$. The filtrate was evaporated under vacuum and the product dissolved in minimal volumes of warm $CHCl_3$. A saturated solution was placed on ice and re-crystallization induced. The resulting product was removed by filtration under vacuum, washed with cold $CHCl_3$ and dried overnight: the dry product was weighed and total yield calculated.

Re-crystallization of the three **NoxF** compounds **NopF**, **NomF** and **NooF** using *iso*-propanol provided higher purity fractions.

Fig. 1. Schematic diagram of the **NxxF** reactions.

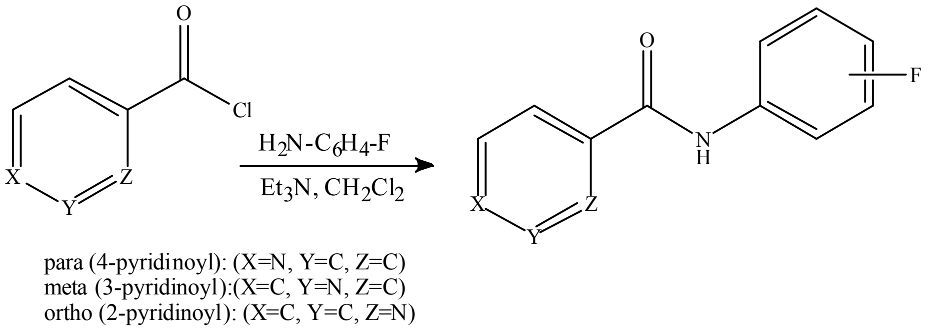

NxxF	m/g	yield/%	mp/°C
NppF	1.059	47	135.0-136.5
NmpF	1.556	69	131.2-133.6
NpoF	1.000	44	139.0-140.0
NmpF	0.750	33	131.5-133.8
NmmF	1.352	60	121.2-122.6
NmoF	1.261	56	116.7-118.2
NopF	0.823	18	92.0-96.0
NomF	0.451	20	77.2-78.0
NooF	0.653	29	105.0-108.0

2. NMR data and spectra

2.1 NppF

^{1}H-NMR (CDCl$_3$): δ 7.11 (2H, t, ^{3}J = 8.5), 7.63 (2H, dd, ^{3}J = 8.9, ^{4}J = 4.7), 7.72 (2H, dd, ^{3}J = 4.5, ^{4}J = 1.5), 7.91 (1H, s), 8.83 (2H, d, J = 5.8); **^{1}H-NMR (DMSO-d$_6$):** δ 7.21 (2H, t, J = 9), 7.80 (2H, dd, ^{3}J = 9.1, ^{4}J = 5.1), 7.86 (2H, dd, ^{3}J = 4.4, ^{4}J = 1.6), 8.79 (2H, dd, ^{3}J = 4.4, ^{4}J = 1.6), 10.65 (1H, s, NH); **^{13}C NMR (DMSO-d_6)** δ 115.17/115.39, 121.52, 122.28/122.36, 134.91, 141.75, 150.22, 157.34/159.73, 163.85; ^{19}F NMR (DMSO-d_6) δ -118.1.

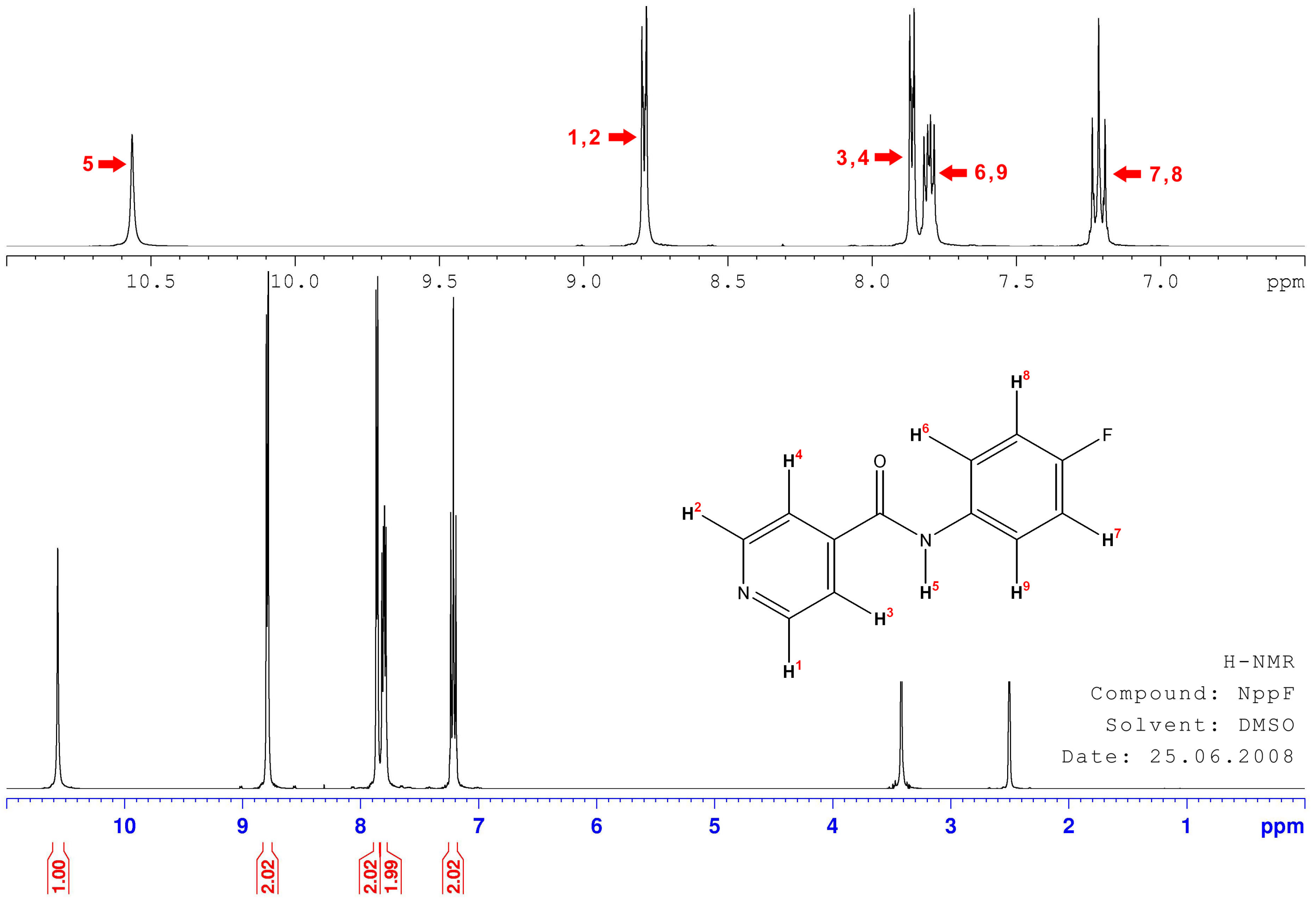

2.2 NpmF

^{1}H NMR (CDCl$_3$) δ 6.92 (1H, tdd, ^{3}J = 8.2, ^{4}J = 2.5, ^{5}J = 1), 7.30 (1H, dq, ^{3}J = 7.8, ^{4}J = 1), 7.36 (1H, td, ^{3}J = 8.1, ^{4}J = 6.2), 7.64 (1H, dt, ^{3}J = 10.6, ^{4}J = 2.1), 7.72 (2H, dd, ^{3}J = 4.4, ^{4}J = 1.6), 8.03 (1H, s), 8.82 (2H, dd, ^{3}J = 4.5, ^{4}J = 1.5); **^{1}H NMR (DMSO-*d*$_6$)** δ 6.97 (1H, tdd, ^{3}J = 8.5, ^{4}J = 2.6, ^{5}J = 1), 7.41 (1H, td, ^{3}J = 8.2, ^{4}J = 6.8), 7.57 (1H, dq, ^{3}J = 8.2, ^{4}J = 1), 7.75 (1H, dt, ^{3}J = 11.6, ^{4}J = 2.3), 7.86 (2H, dd, ^{3}J = 4.4, ^{4}J = 1.6), 8.80 (2H, dd, ^{3}J = 4.2, ^{4}J = 1.8), 10.68 (1H, s); **^{13}C NMR (DMSO-*d*$_6$)** δ 107.00/107.25, 110.52/110.73, 116.10, 121.53, 130.26/130.36, 140.25/140.36, 141.58, 150.25, 160.80/163.20, 164.25; **^{19}F NMR (DMSO-*d*$_6$)** δ -112.0.

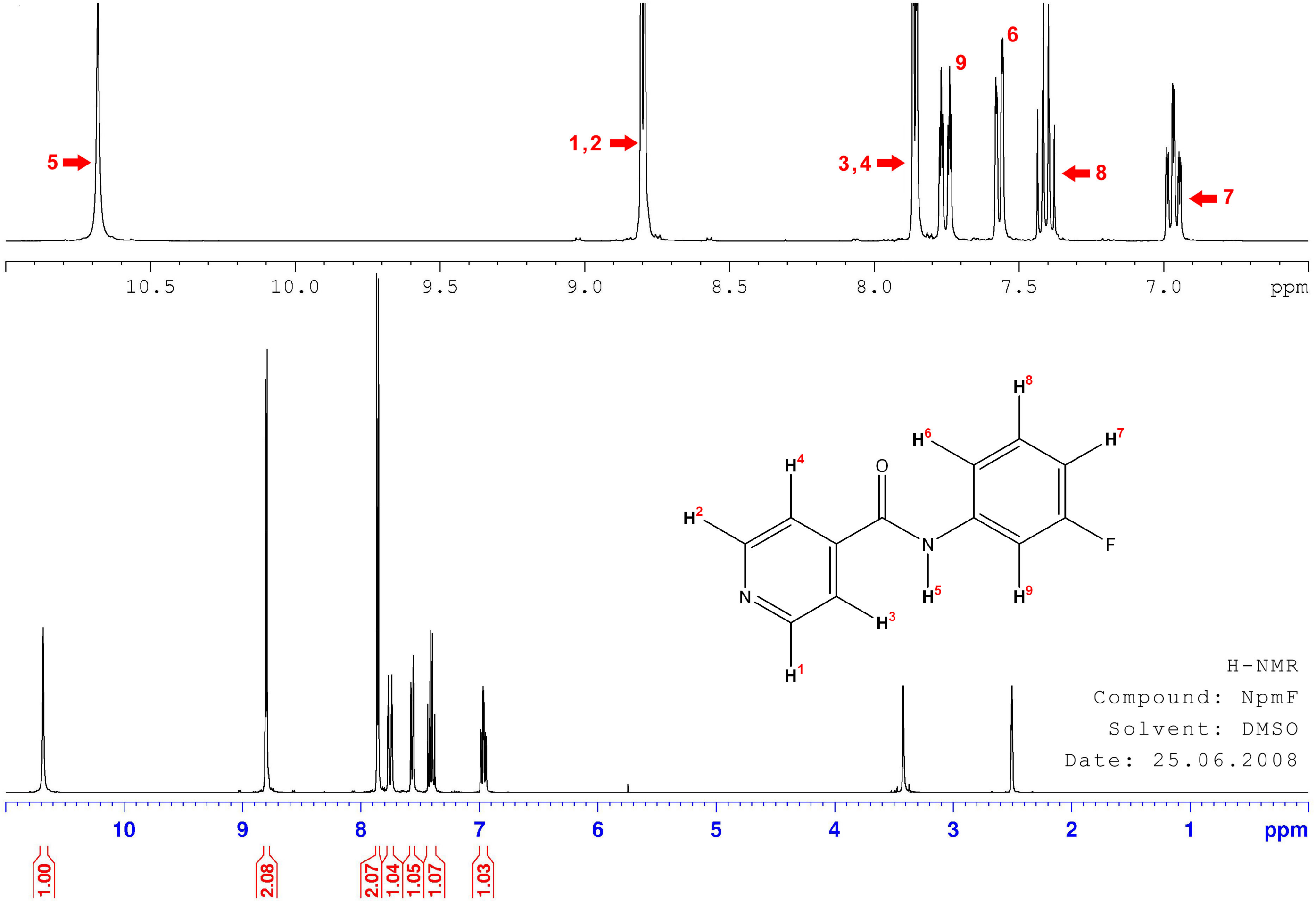

2.3 NpoF

^{1}H NMR (CDCl$_3$) δ 7.16 (1H, td), 7.18 (1H, td), 7.23 (1H, td), 7.75 (2H, dd, ^3J = 4.4, ^4J = 1.6), 8.15 (1H, s), 8.44 (1H, td, ^3J = 8), 8.84 (2H, dd, ^3J = 4.4, ^4J = 1.6); **^{1}H NMR (DMSO-d_6)** δ 7.24 (1H, td), 7.30 (1H, td), 7.31 (1H, td), 7.64 (1H, td, ^3J = 7.7, ^4J = 1), 7.89 (2H, dd, ^3J = 4.5, ^4J = 1.6), 8.80 (2H, dd, ^3J = 4.4, ^4J = 1.7), 10.45 (1H, s); **^{13}C NMR (DMSO-d_6)** δ 115.80/115.99, 121.60, 124.37, 124.99/125.11, 127.09, 127.35/127.43, 140.90, 150.32, 154.50/156.95, 164.00; **^{19}F NMR (DMSO-d_6)** δ -121.0.

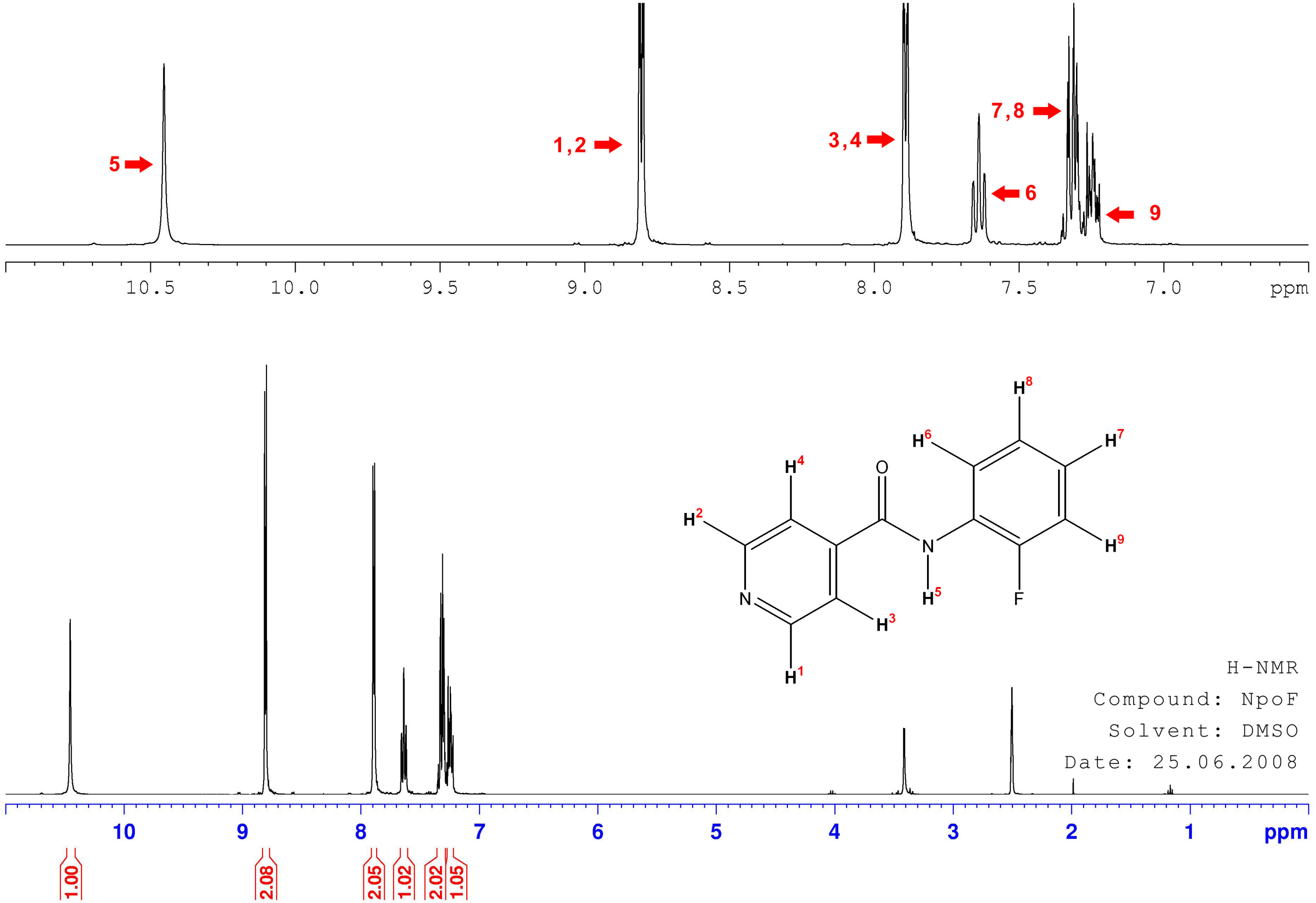

2.4. NmpF

^{1}H NMR (CDCl$_3$) δ 6.98 (2H, t, $J = 8.6$), 7.35 (1H, ddd, $^{3}J = 7.9$, $^{3}J = 4.9$, $^{5}J = 0.7$), 7.53 (2H, dd, $^{3}J = 8.9$, $^{4}J = 4.7$), 8.13 (1H, dt, $^{3}J = 7.9$, $^{4}J = 3.8$), 8.44 (1H, s), 8.65 (1H, dd, $^{3}J = 4.9$, $^{4}J = 1.6$), 9.02 (1H, d, $^{4}J = 1.8$); **^{1}H NMR (DMSO-d_6)** δ 7.21(2H, $J = 8.9$), 7.57 (1H, ddd, $^{3}J = 8$, $^{3}J = 4.8$, $^{5}J = 0.7$), 7.80 (2H, dd, $^{3}J = 9.2$, $^{4}J = 5$), 8.29 (1H, dt, $^{3}J = 8$, $^{4}J = 2$), 8.77 (1H, dd, $^{3}J = 4.8$, $^{4}J = 1.6$), 9.12 (1H, d, $^{4}J = 2.2$), 10.50 (1H, s); **^{13}C NMR (DMSO-d_6)** δ 115.13/115.36, 122.14/122.22, 123.46, 130.41, 135.16, 135.39, 148.62, 152.10, 157.21/159.60, 163.93; **^{19}F NMR (DMSO-d_6)** δ -118.4.

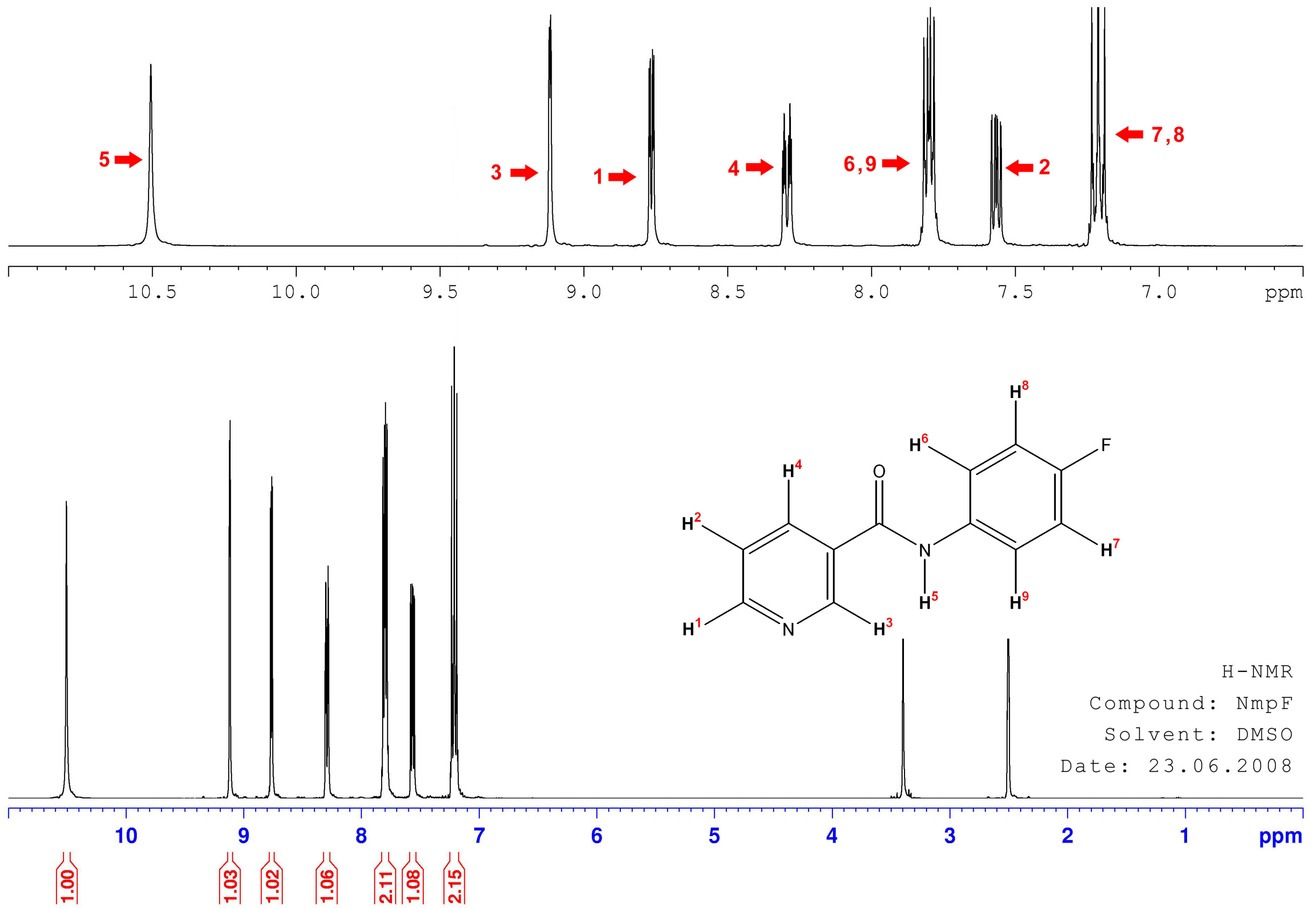

2.5. NmmF

^{1}H NMR (CDCl$_3$) δ 6.88 (H1, tdd, $^{3}J = 7.7$, $^{4}J = 2.5$, $^{5}J = 1.5$), 7.29 (1H, dd, $^{3}J = 5.8$, $^{4}J = 2.7$), 7.33 (1H, td, $^{3}J = 4.4$), 7.42 (1H, ddd, $^{3}J = 8.1$, $^{3}J = 4.9$, $^{5}J = 0.7$), 7.61 (1H, dt, $^{3}J = 10.7$, $^{4}J = 2.1$), 8.21 (1H, dt, $^{3}J = 8$, $^{4}J = 2$), 8.72 (1H, dd, $^{3}J = 4.9$, $^{4}J = 1.6$), 8.75 (1H, s), 9.09 (1H, d, $^{4}J = 2.2$); **^{1}H NMR (DMSO-*d*$_6$)** δ 6.95 (1H, td, $^{3}J = 8.4$, $^{4}J = 2.5$), 7.40 (1H, td, $^{3}J = 8.2$, $^{4}J = 7$), 7.56 (1H, dd), 7.57 (1H, ddd), 7.76 (1H, dt, $^{3}J = 11.7$, $^{4}J = 2.3$), 8.30 (1H, dt, $^{3}J = 8$, $^{4}J = 2$), 8.78 (1H, dd, $^{3}J = 4.8$, $^{4}J = 1.6$), 9.12 (1H, d, $^{4}J = 2.2$), 10.62 (1H, s); **^{13}C NMR (DMSO-*d*$_6$)** δ 106.84/107.10, 110.28/110.49, 115.94/115.96, 123.47, 130.23/130.28, 130.33, 135.49, 140.51/140.62, 148.67, 152.25, 160.81/163.21, 164.31; **^{19}F NMR (DMSO-*d*$_6$)** δ -112.1.

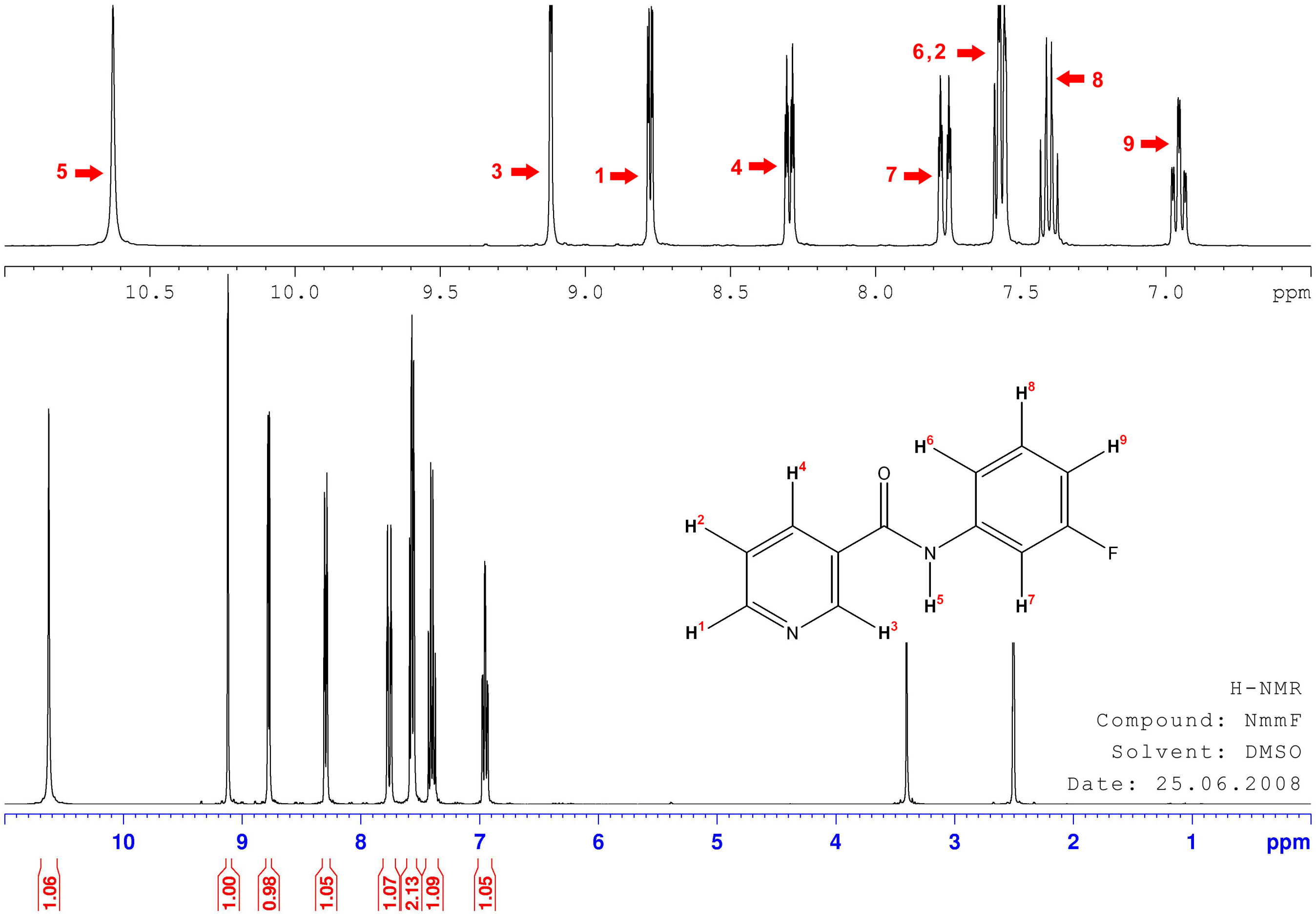

2.6. NmoF

^{1}H NMR ($CDCl_3$) δ 7.15 (1H, td), 7.17 (1H, td), 7.21 (1H, td), 7.48 (1H, ddd, ^3J = 8, ^3J = 4.8, ^5J = 0.7), 8.23 (1H, s), 8.24 (1H, dt, ^3J = 7.9, ^4J = 2), 8.39 (1H, t, ^3J = 8), 8.80 (1H, dd, ^3J = 4.8, ^4J = 1.6), 9.14 (1H, ^3J = 1.8); **^{1}H NMR (DMSO-d_6)** δ 7.25 (1H, td, ^3J = 7, ^4J = 2.4), 7.30 (1H, td), 7.32 (1H, td), 7.58 (1H, ddd, ^3J = 8, ^3J = 4.8, ^5J = 0.7), 7.65 (1H, td, ^3J = 7.8, ^4J = 1.4), 8.32 (1H, dt, ^3J = 8, ^4J = 2), 8.78 (1H, dd, ^3J = 4.8, ^4J = 1.6), 9.15 (1H, ^3J = 1.9), 10.38 (1H, s); **^{13}C NMR (DMSO-d_6)** δ 115.77/115.96, 123.52, 124.33/124.36, 125.22/125.35, 127.00, 127.12/127.20, 129.56, 135.54, 148.79, 152.34, 156.88/154.43, 164.07; **^{19}F NMR (DMSO-d_6)** δ -121.1.

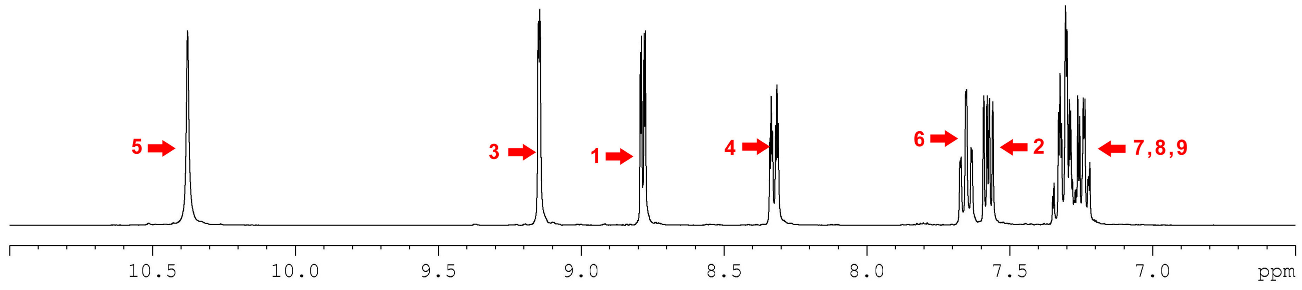

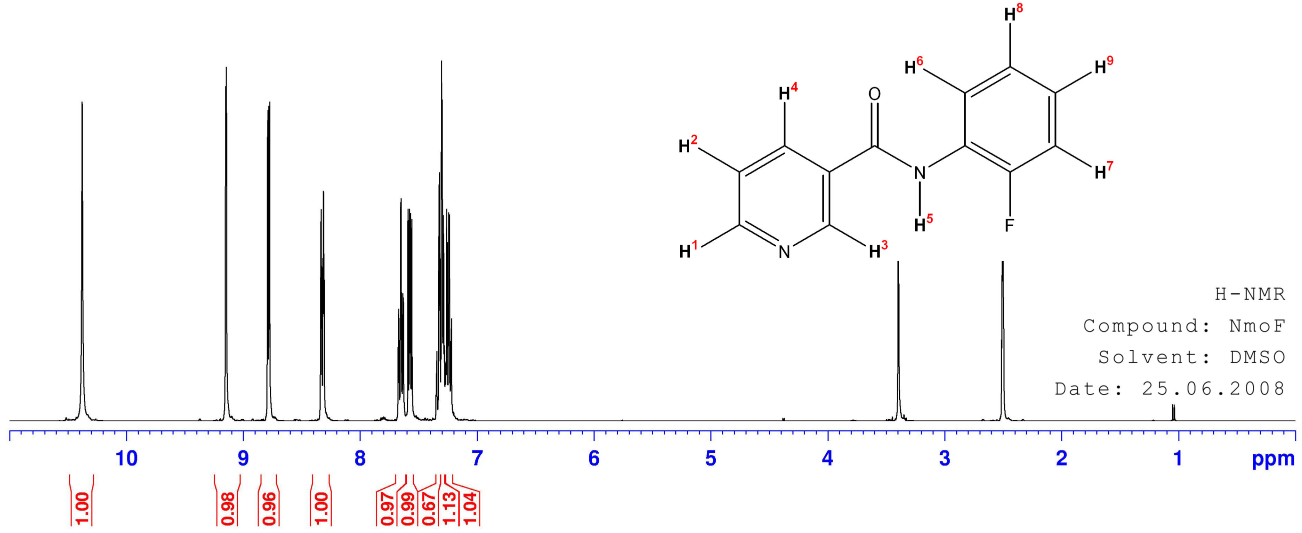

2.7. NopF

^{1}H NMR (CDCl$_3$): δ 7.09 (2H, t, J = 8.7), 7.50 (1H, dd, ^3J = 7.9, ^4J = 4.8), 7.77 (2H, dd, ^3J = 9.1, ^4J = 4.8), 7.93 (1H, td, ^3J = 7.7, ^4J = 1.6), 8.31 (1H, d, ^3J = 7.8), 8.62 (1H, d, ^3J = 4.5), 10.04 (1H, s); **^{1}H NMR (DMSO-*d*$_6$)**: δ 7.19 (2H, t, J = 8.9), 7.66 (1H, dd, ^3J = 7.6, ^4J = 4.7), 7.95 (2H, dd, ^3J = 9.1, ^4J = 5.1), 8.05 (1H, td, ^3J = 7.7, ^4J = 1.3), 8.16 (1H, d, ^3J = 7.8), 8.73 (1H, d, ^3J = 4.6), 10.74 (1H, s); **^{13}C NMR (DMSO-*d*$_6$)**: δ 115.05/115.27, 122.08/122.16, 122.37, 126.86, 134.76, 138.05, 148.35, 149.77, 157.19/159.59, 162.43; **^{19}F NMR (DMSO-*d*$_6$)**: δ -118.5.

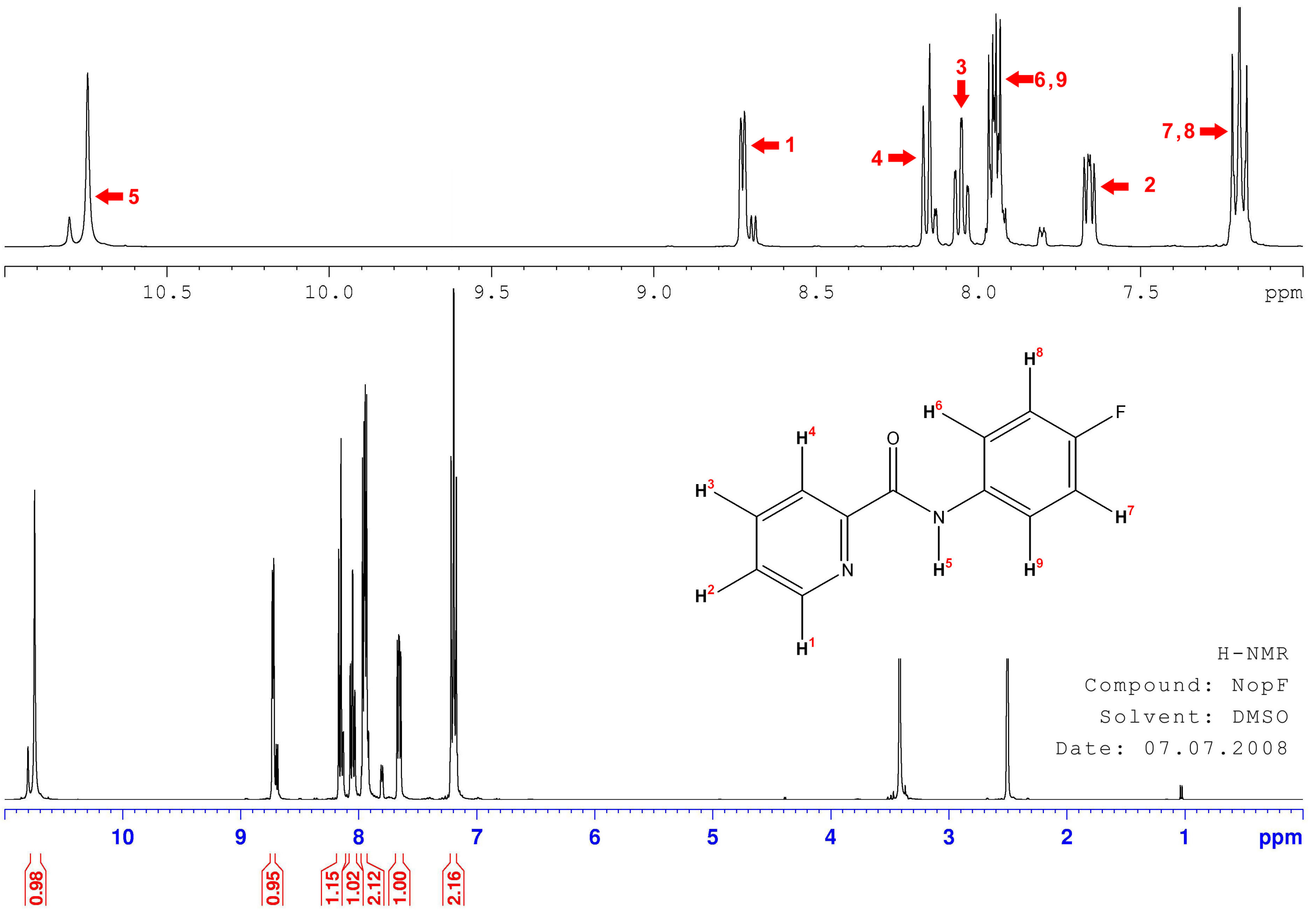

2.8 NomF

^{1}H NMR (CDCl$_3$): δ 6.86 (1H, tdd, $^3J = 8.3$, $^4J = 2.5$, $^5J = 1$), 7.34 (1H, td, $^3J = 8.1$, $^4J = 6.4$), 7.42 (1H, dq, $^3J = 8.1$, $^4J = 1$), 7.52 (1H, ddd, $^3J = 7.6$, $^4J = 4.8$, $^5J = 1.2$), 7.79 (1H, dt, $^3J = 11$, $^4J = 2.2$), 7.94 (1H, td, $^3J = 7.7$, $^4J = 1.7$), 8.31 (1H, dt, $^3J = 7.8$, $^4J = 1$), 8.63 (1H, dq, $^3J = 4.8$, $^4J = 0.8$), 10.13 (1H, s); **^{1}H NMR (DMSO-*d*$_6$)**: δ 6.94 (1H, tdd, $^3J = 8.8$, $^4J = 2.5$, $^5J = 0.8$), 7.39 (1H, td, $^3J = 8.2$, $^4J = 7$), 7.68 (1H, ddd, $^3J = 7.8$, $^4J = 4.8$, $^5J = 1.2$), 7.76 (1H, dq, $^3J = 8.3$, $^4J = 1$), 7.90 (1H, dt, $^3J = 11.8$, $^4J = 2.3$), 8.07 (1H, td, $^3J = 7.7$, $^4J = 1.7$), 8.17 (1H, d, $^3J = 7.8$), 8.74 (1H, dq, $^3J = 4.8$, $^4J = 0.8$), 10.86 (1H, s); **^{13}C NMR (DMSO-*d*$_6$)**: δ 106.87/107.13, 110.22/110.43, 116.07/116.09, 122.50, 127.05, 130.15/130.25, 138.12, 140.07/140.18, 148.40, 149.53, 162.78, 160.83/163.23; **^{19}F NMR (DMSO-*d*$_6$)** δ -112.1.

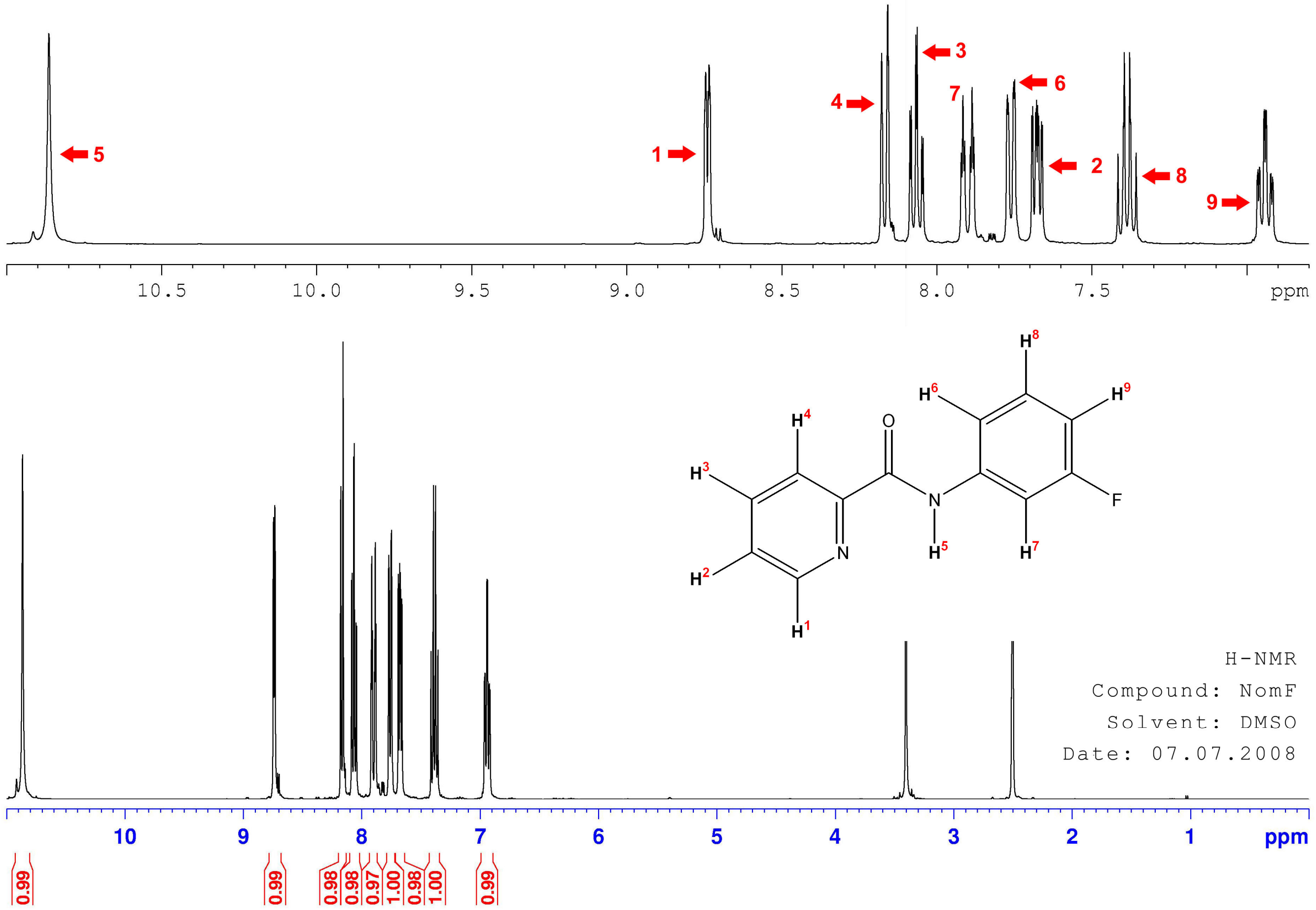

2.9 NooF

^{1}H NMR (CDCl$_3$) δ 7.11 (1H, td), 7.15 (1H, td), 7.19 (1H, td), 7.51 (1H, ddd, $^3J = 7.5$, $^4J = 4.8$, $^5J = 1.2$), 7.92 (1H, td, $^3J = 7.7$, $^4J = 1.7$), 8.31 (1H, dt, $^3J = 7.8$, $^4J = 1$), 8.60 (1H, td, $^3J = 8.1$, $^4J = 1.6$), 8.66 (1H, dq, $^3J = 4.7$, $^4J = 0.9$), 10.36 (1H, s,); **^{1}H NMR (DMSO-d$_6$)** δ 7.21 (1H, td), 7.22 (1H, td), 7.32 (1H, td, $^3J = 9.5$, $^4J = 1.8$), 7.68 (1H, ddd, $^3J = 7.6$, $^4J = 4.7$, $^5J = 1.2$), 8.07 (1H, td, $^3J = 7.7$, $^4J = 1.7$), 8.16 (1H, d, $^3J = 7.7$), 8.17 (1H, td, $^3J = 8$, $^4J = 2$), 8.72 (1H, dq, $^3J = 4.5$, $^4J = 0.7$), 10.37 (1H, s); **^{13}C NMR (DMSO-d$_6$)** δ 115.27/115.46, 122.17, 122.85, 124.55/124.59, 125.48/125.40, 125.58/125.70, 127.25, 138.28, 148.55, 148.79, 154.71/152.28, 161.86; **^{19}F NMR (DMSO-*d*$_6$)** δ -127.4.

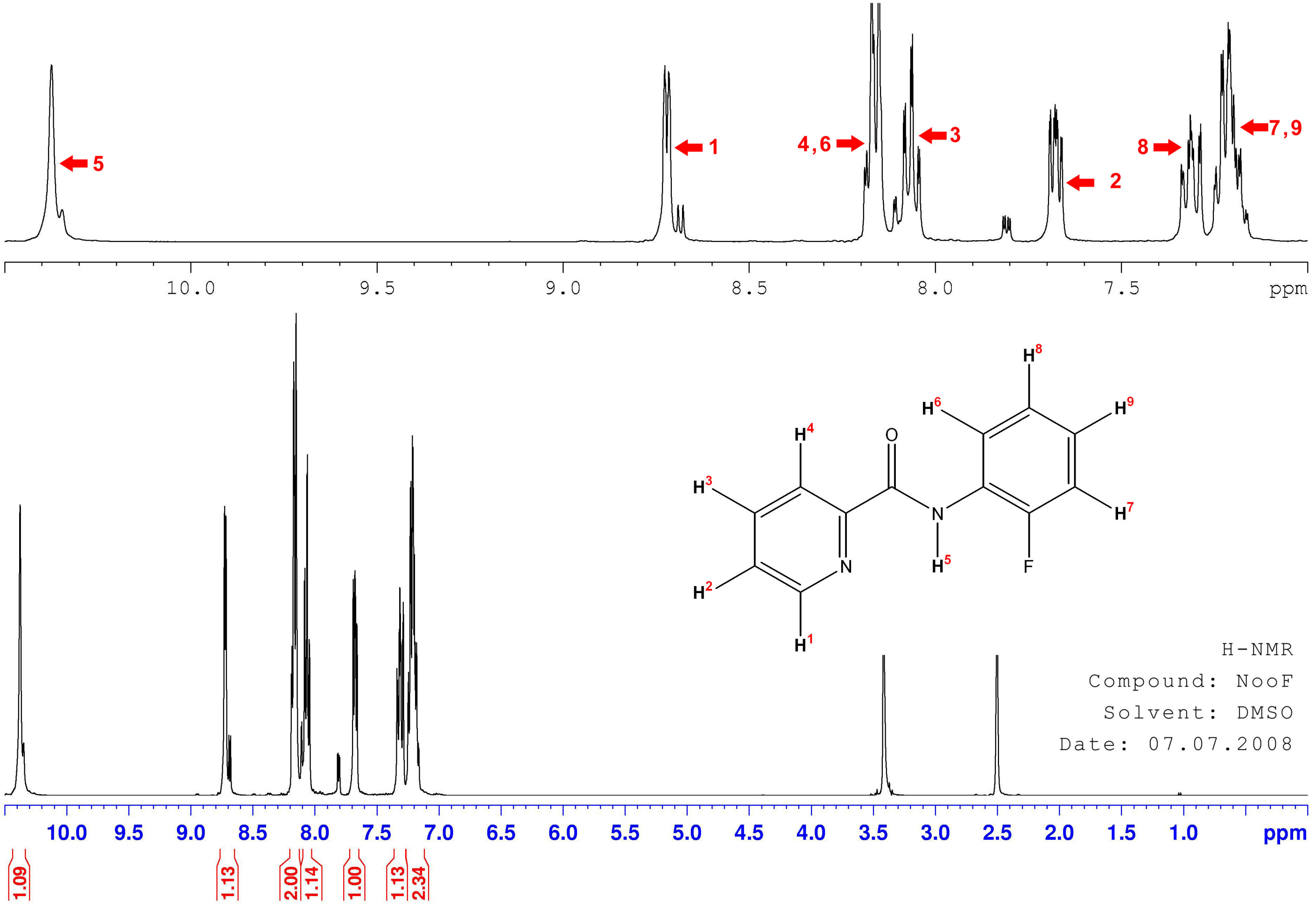

3. IR (KBr disc)

3.1. NppF

3354 (N-H stretch), 1651 (C=O stretch).

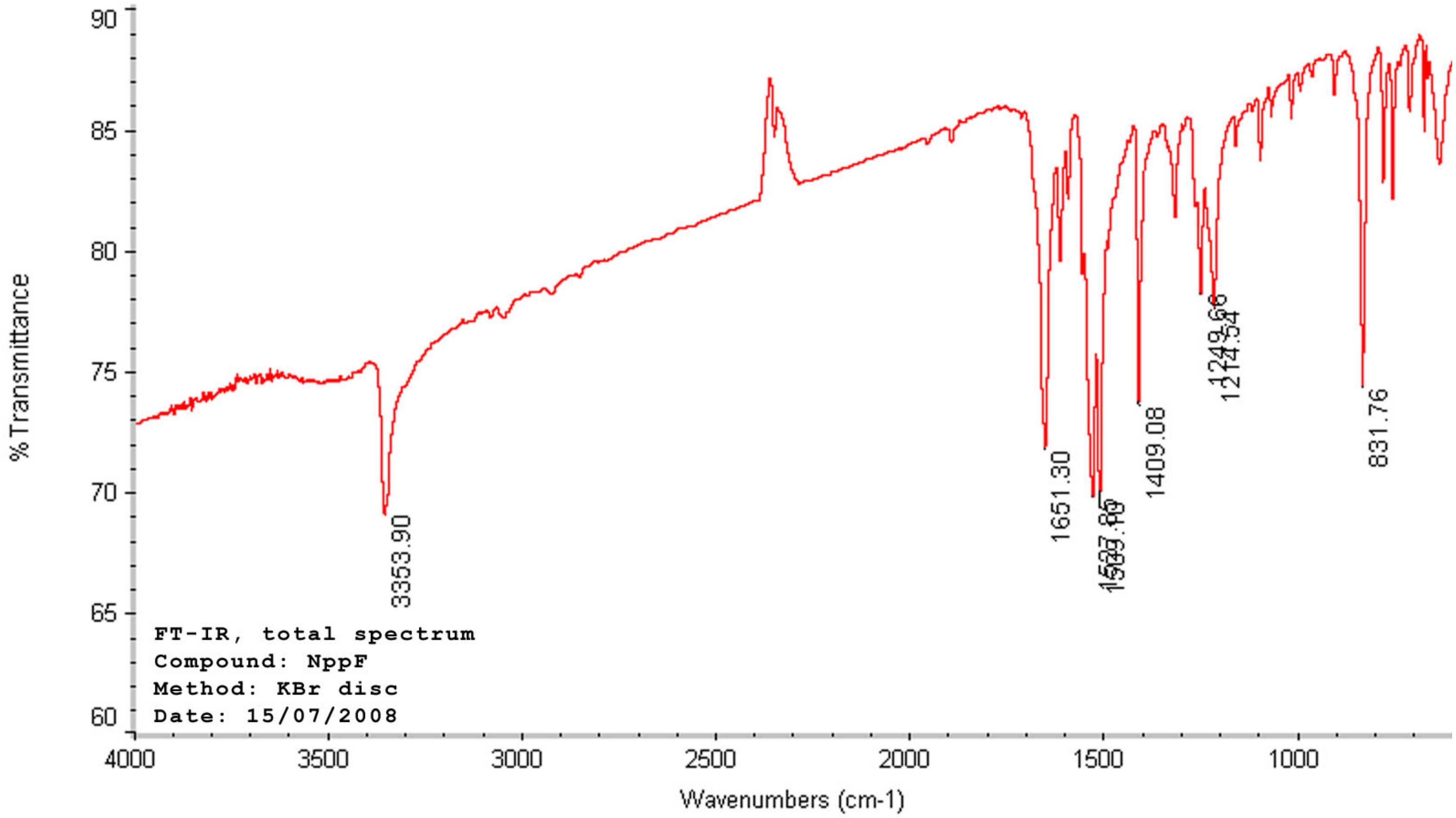

Supplementary Material (ESI) for CrystEngComm

3.2. NpmF

3456/3193 (N-H stretch), 1690/1676 (C=O stretch).

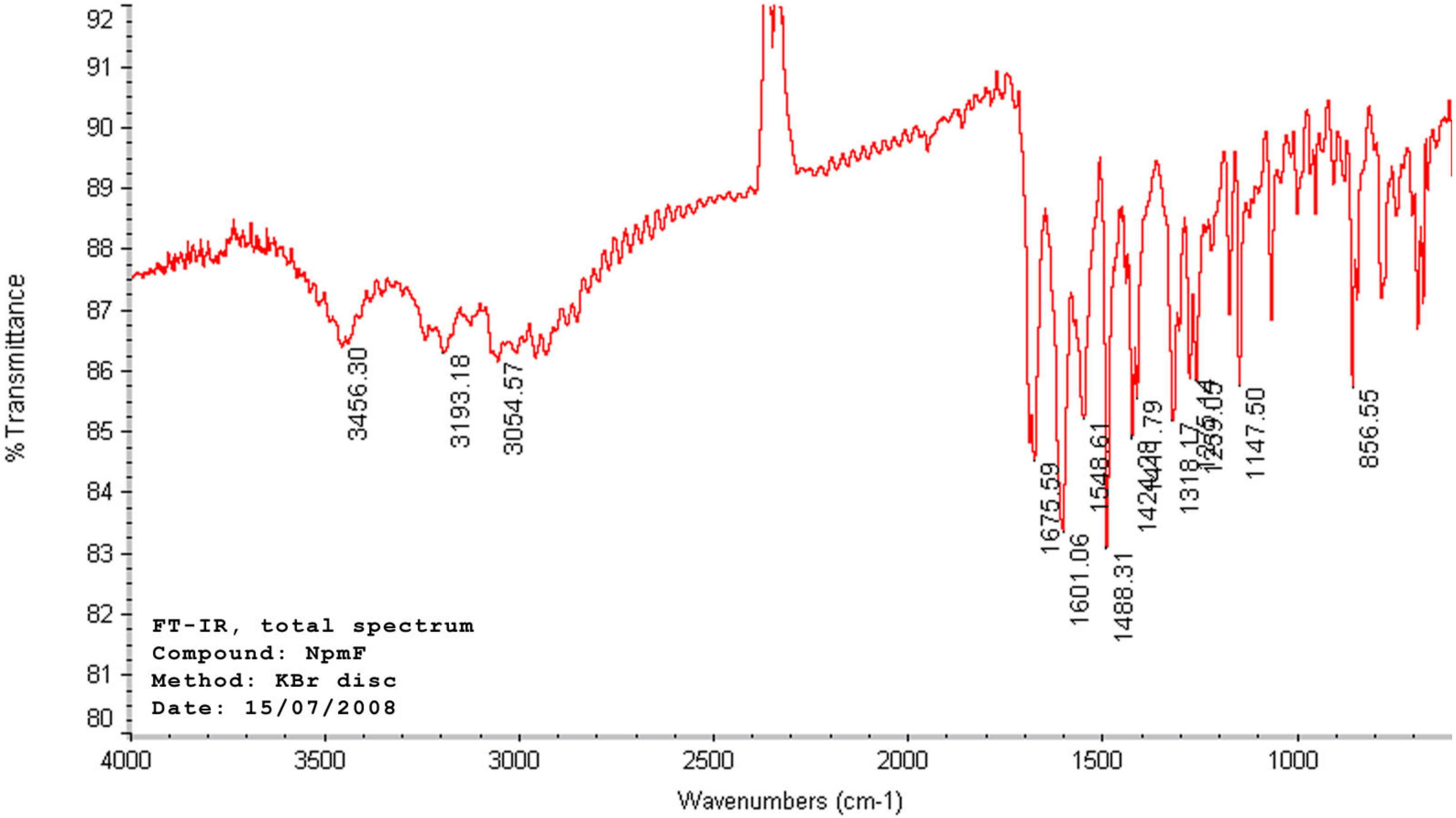

3.3. NpoF

3180 (N-H stretch), 1694/1679 (C=O stretch).

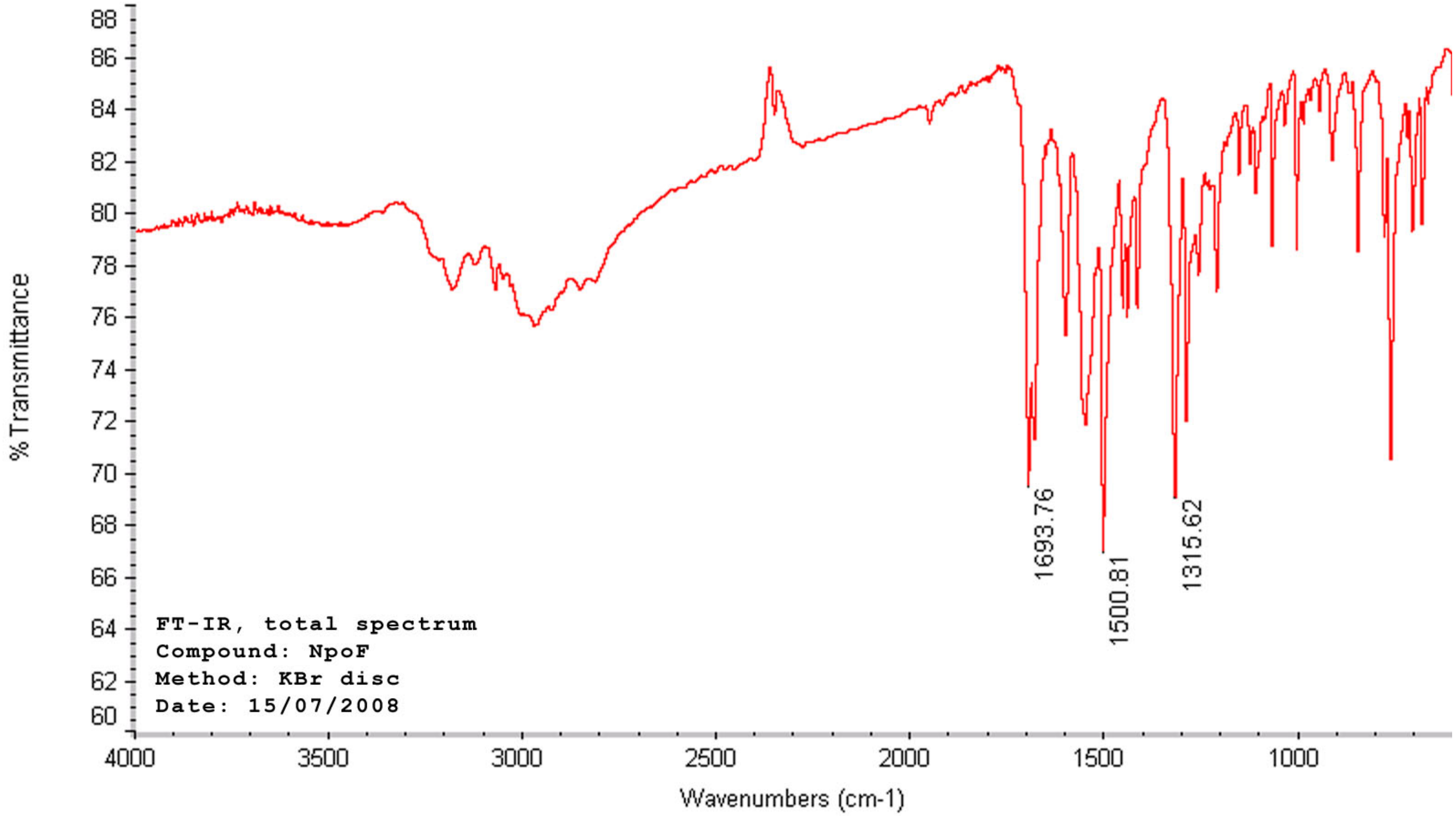

3.4. NmpF

3321 (N-H stretch), 1682 (C=O stretch).

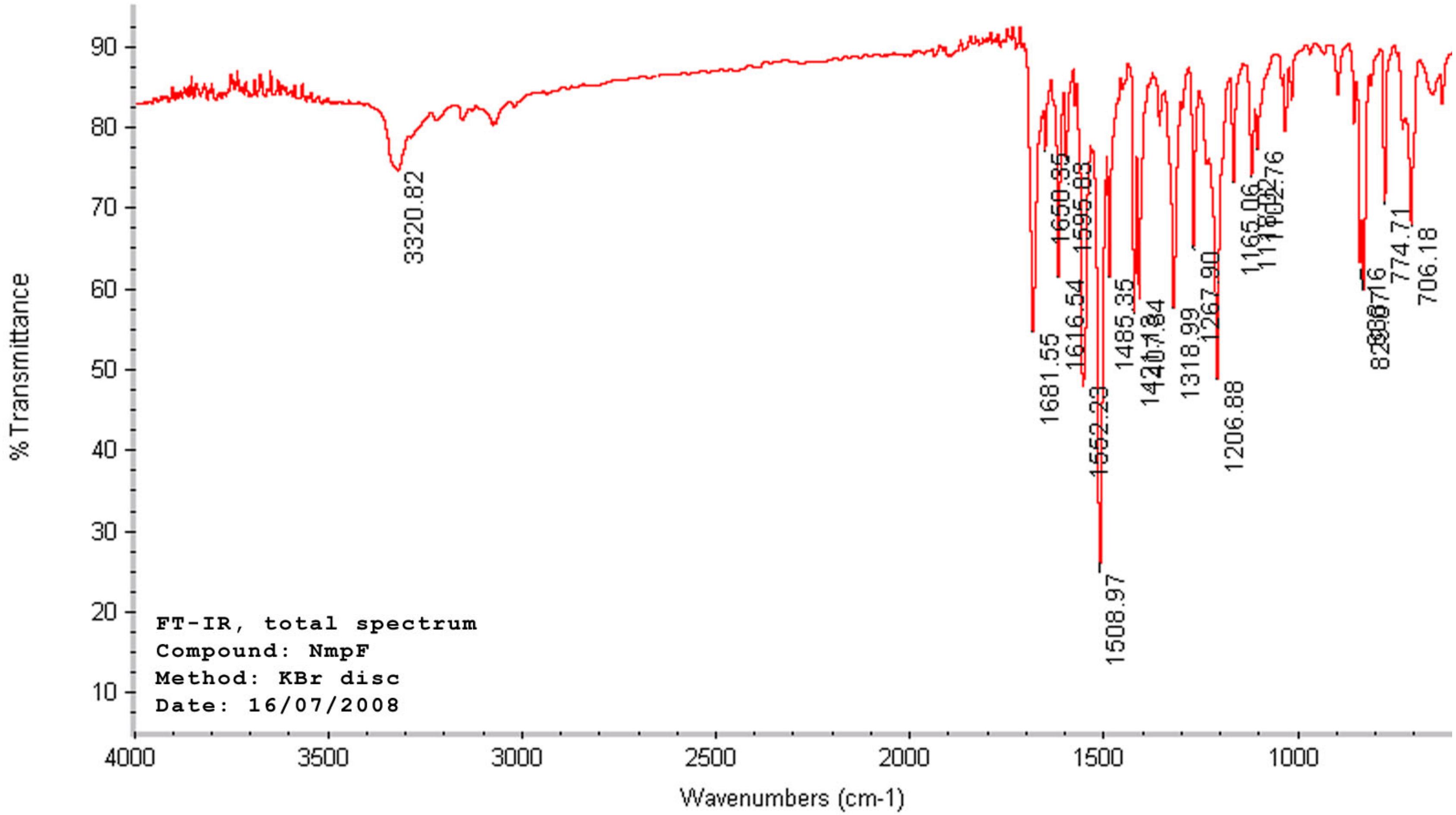

3.5. NmmF

3258 (N-H stretch), 1681 (C=O stretch).

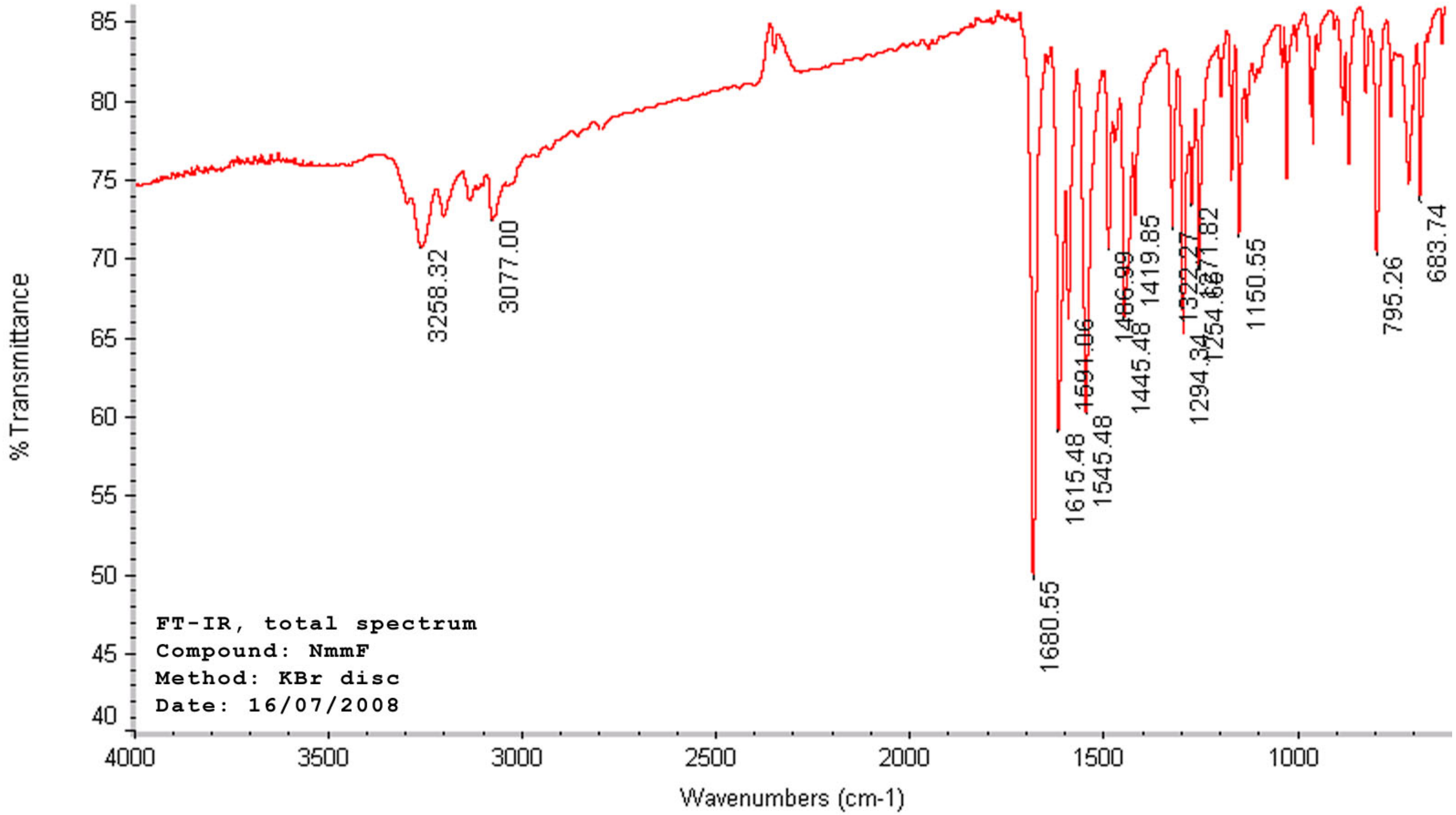

3.6. NmoF

3295 (N-H stretch), 1679 (C=O stretch).

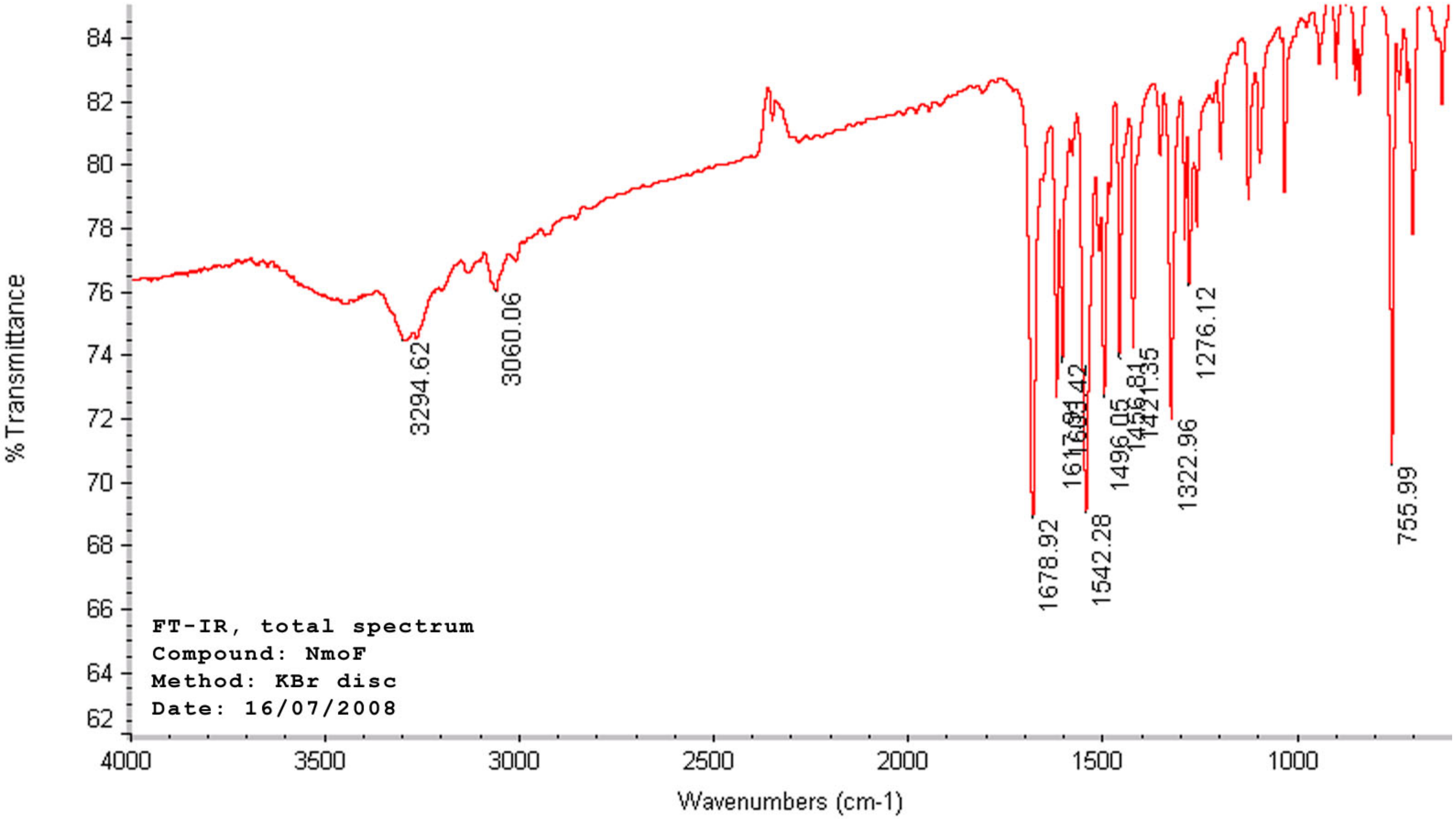

3.7. NopF

3342 (N-H stretch), 1683 (C=O stretch).

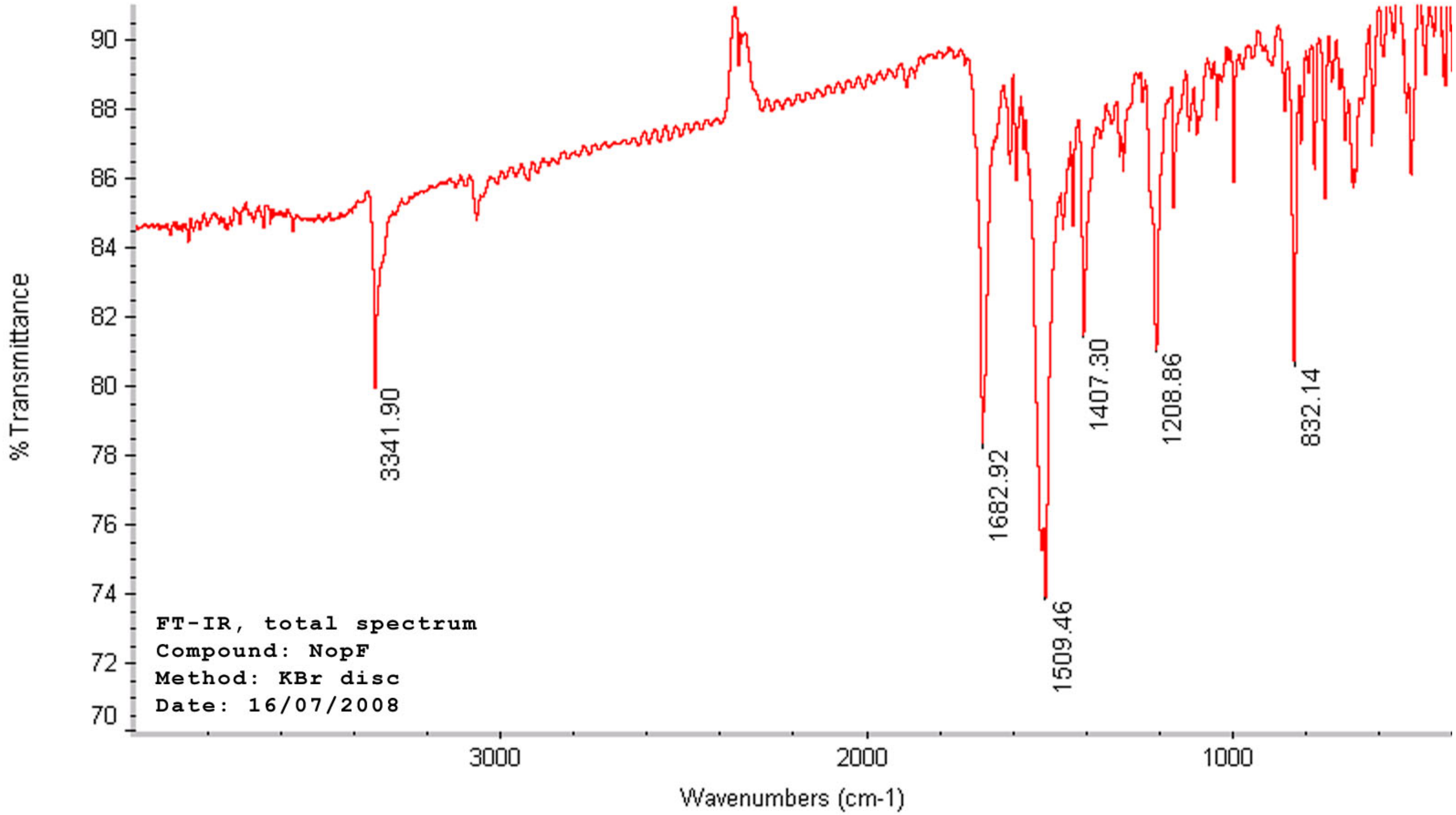

3.8. NomF

3332 (N-H stretch), 1684 (C=O stretch).

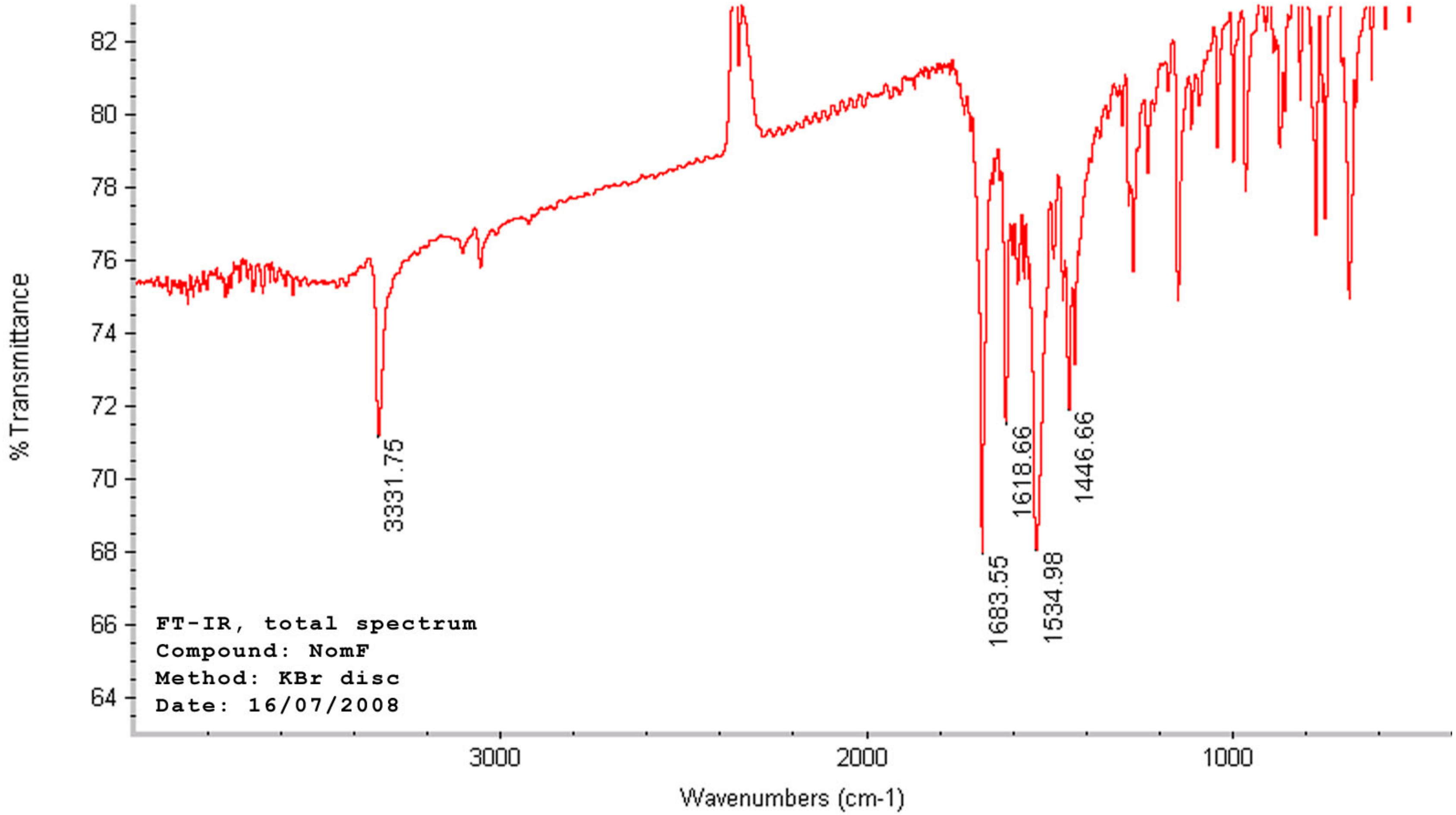

3.9. NooF

3333 (N-H stretch), 1689 (C=O stretch).

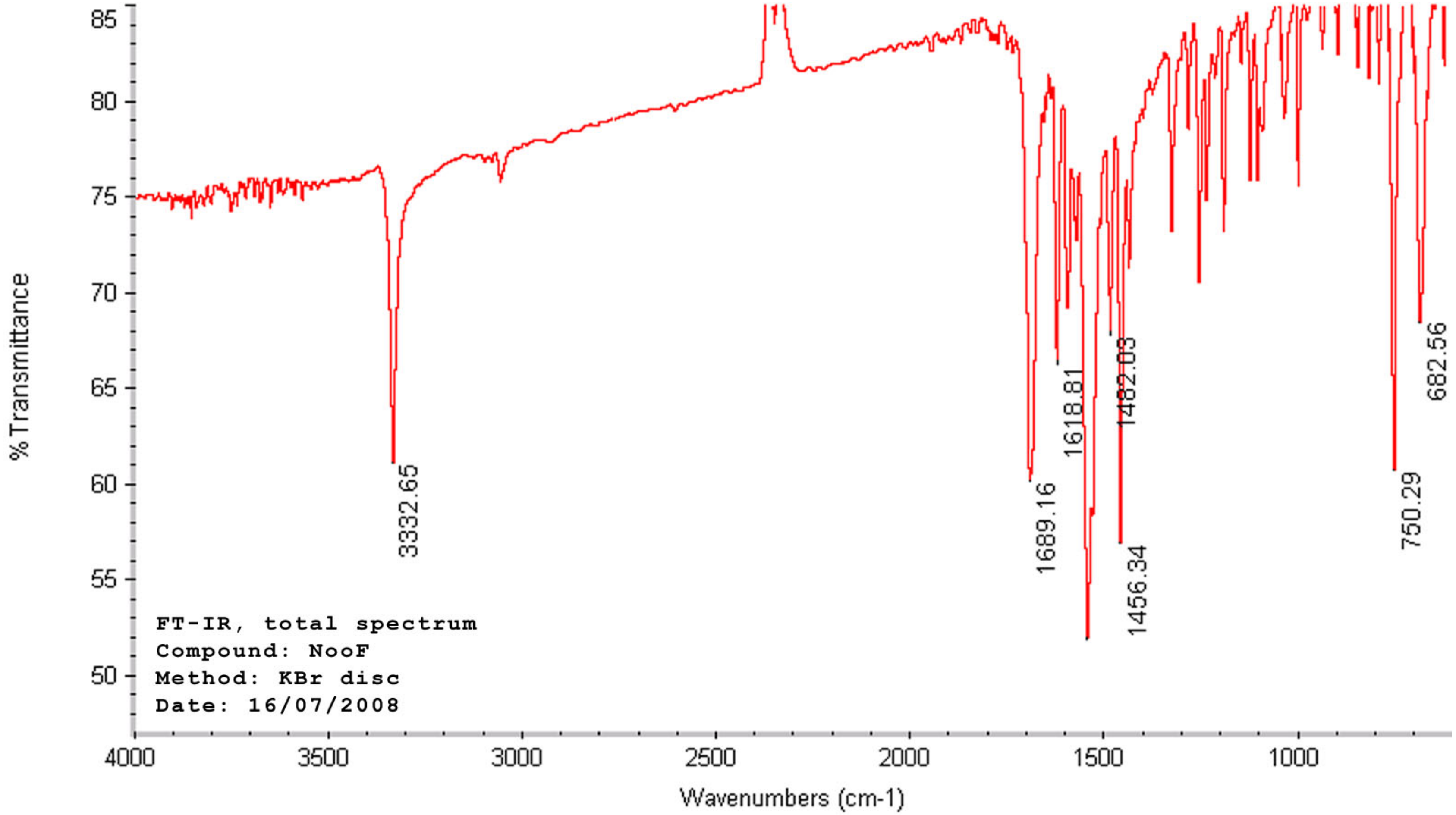

4. Crystallographic details for nine NxxF compounds.

NxxF molecular and crystal structure data

The distinct intermolecular feature for eight of the **NxxF** crystal structures (where **x** = *para-*/*meta-*/*ortho*) is that they aggregate in the solid-state *via* $_{\text{amide}}$N-H…N$_{\text{pyridine}}$ hydrogen bonds, but in different crystal systems and space groups. The **NppF** isomer is the only **NxxF** structure where the primary hydrogen bonding is *via* N-H…O=C* interactions. Of the nine **NxxF** structures there are only three, **NpmF**, **NmmF** and **NmoF** that crystallize with *Z'*=1 and with no disorder: the remaining six **NxxF** crystallize with one of more of the following: (*i*) more than one molecule in the asymmetric unit, (*ii*) disorder in the orientation of the C_6H_4F ring and/or (*iii*) have a minor Cl component of impurity (derived from the original NoxF synthesis). The **NmpF** structure is of further interest as it forms a $_{\text{amide}}$N-H…N$_{\text{pyridine}}$ hydrogen bonded tetrameric assembly (with C-H...N) and further linked by C-H…F and C-H…O=C interactions.
* - refers to **Table 2** of the main paper and that **NppF** is the only **NxxF** structure with amide...amide assembly.

4.1 NpxF structure series of NppF, NpmF and NpoF

The three **NpxF** compounds aggregate *via* two different primary hydrogen bonding intermolecular interactions (*i.e.* the typical amide…amide as N-H…O=C for **NppF** and N-H…N$_{\text{pyridine}}$ for **NpmF**, **NpoF**; the latter two are isomorphous).

4.1.1 NppF molecular and crystal structure [9-08]

The **NppF** crystal structure crystallizes in $P\,\bar{1}$ (No. 2) with *Z'*=2; data were collected at 200(1) K. The crystal and molecular structure solution of **NppF** is quite interesting in that quality crystals analysed at 150(1) K would not yield a solution: therefore by increasing the temperature to 200(1) K a meaningful result was obtained whereby the unit cell was halved. It is a non-merohedral twinned crystal with two components of 0.89:0.11. Metrically, it suggests a unit cell change to the monoclinic system but this does not seem appropriate for the results at 200(1) K. There are several distinct differences between the two independent (A) and (B) molecules in the asymmetric unit; an example is the F14$_{A/B}$...N24$_{A/B}$ intramolecular distance between the F and pyridine-N atoms of 9.800(3) in (A) and 9.769(3) Å in (B).

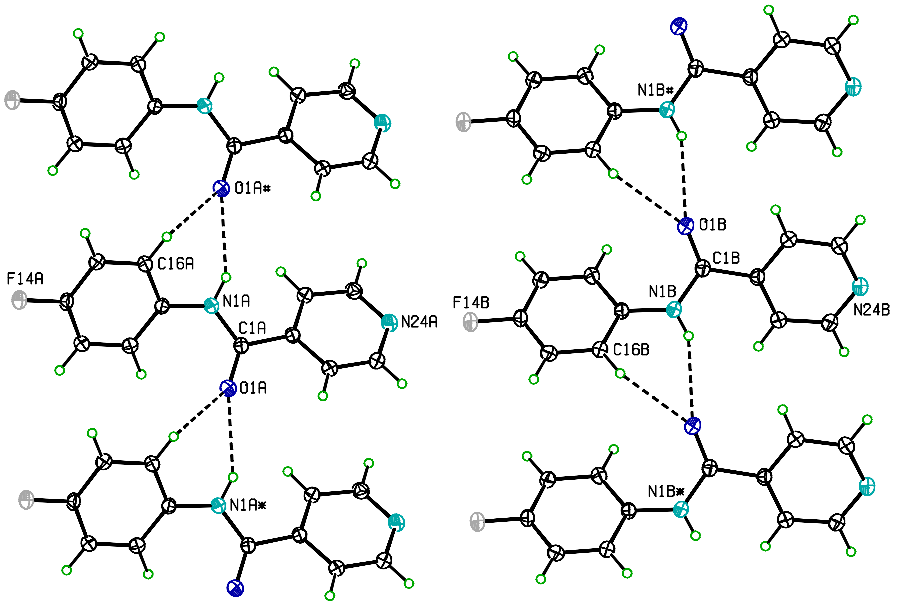

Figure 1 An ORTEP diagram of the N-H...O=C and C-H…O=C interactions in **NppF** with displacement ellipsoids drawn at the 30% probability level. The symmetry codes # and * refer to 1+x,y,z and x-1,y,z, respectively.

The molecules aggregate along the *a*-axis [100] direction as amide N-H…O=C* chains [*C*(4) chains] with rather long intermolecular distances of 3.203(2) and 3.216(2) Å for molecules (A) and (B), respectively, and in tandem with this is a rather weak C16-H16$_{A/B}$…O1$_{A/B}$ contact forming $R^1_2(6)$ rings, together with an intramolecular C-H…O contact (**Figure 1**). The molecules aggregate as weakly interacting A…A.., and B…B… chains with similar N…O distances (the aggregation is principally 1D). Interestingly, the pyridine N24(A/B) atoms do not participate in hydrogen bonding or even in weak contacts (which is unusual). The two *para*-fluorine atoms [F14$_{A/B}$] form contacts and interact with symmetry related fluoro atoms with F…F distances of 2.86 Å, some 0.10 Å < van der Waals contact radii distance: this enables the formation of *zig-zag* chains of F atoms along the *a*-axis direction. The larger two molecule wide columns stack *via* C-H…π(arene) interactions and manifesting as a chain of weakly interacting F atoms along [100].

The aromatic C_6/C_5N interplanar angles in molecules A and B are 56.74(5)° and 57.93(5)°, respectively, and differing by only 1°. However, the biggest angle difference is for the C_6/five-atom amide group and two linker C atoms [C11/C1/O1/N1/C21] and differing by 4° with 29.24(7)° for molecule (A) and 33.16(6)° for molecule (B). Using a structural overlay, it can be observed that the differences are small and in an opposite sense to the amide group. Torsion angle differences of 2-3° in **NppF** are C1-N1-C11-C16 = 150.9(2)° in molecule (A) and = -148.1(2)° in molecule (B).

4.1.2 NpmF molecular and crystal structure [9-17]

The **NpmF** crystal structure (**Figure 2**) is a regular structure with intermolecular N–H…$N_{pyridine}$ interactions and without molecular disorder: the N1…N24 distance is typical at 2.991(4) Å and the aggregation is *via* *C*(7) *zigzag* chains augmented by intermolecular C-H...O=C interactions (*via* C15-H15) and C-H...F contacts [both as $R^1_2(5)$ rings] into 2D sheets; a reasonably short C-H…π(arene) interaction is also present. The arene interaction has a H25…Cg distance of 2.65 Å and with C25…Cg = 3.484(3) Å and a C25-H25…Cg angle of 147° [Cg = ring centroid]. This is not as short as the C-H…π(arene) interaction in the crystal structure of **Moo** [paper reference 12]. The fluorine atoms in **NpmF** do not participate in interactions apart from weak contacts as depicted in Figure 2 below. The angle between the C_6/C_5N planes is 65.93(10)°, whereas the C_5N/amide and C_6/amide are intermediate at 27.39(13)° and 39.16(10)°.

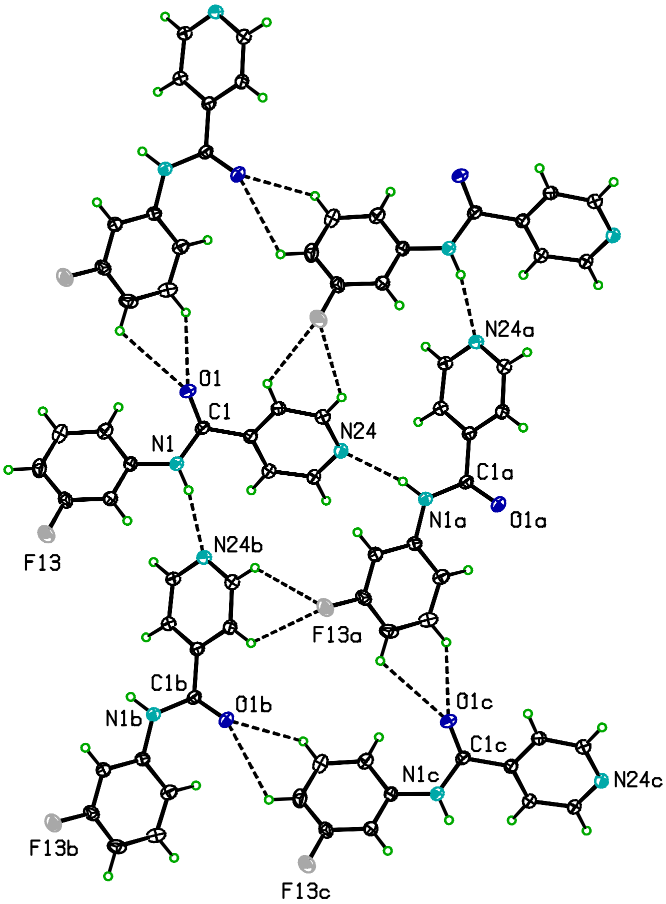

Figure 2 The primary intermolecular interactions in the 2D sheet of **NpmF** comprising N-H...N hydrogen bonds and weaker C-H...O/F interactions/contacts (with displacement ellipsoids depicted as in **Figure 1**). The suffixes *a*, *b* and *c* refer to the symmetry operations of 1/2+x, -1/2-y, 1/2+z; -1/2+x, -1/2-y, -1/2+z and x, y-1, z with two additional molecules showing the repeat. **An extended version of the hydrogen bonding is provided as Figure 2 in the main paper.**

4.1.3. NpoF molecular and crystal structure [9-09]

The **NpoF** structure has C_6 and C_5N aromatic rings that are almost mutually orthogonal at 76.99(12)°. There is a minor component of disorder present in the fluorobenzene at 8.3(9)% and involves a 180° rotation about the N1-C11 axis with H/F atoms interchanging: this type of H/F interchange and disorder is not uncommon. The N…N hydrogen bonding is short and forms a 1D zigzag *C*(7) chain parallel to the $(10\bar{1})$ plane: this N…N distance is shorter when compared to related systems with similar N-H…N interactions *e.g.* as in **NpmF**. The C-H…N contact is rather long and does not augment the primary N-H...N interaction. Two long C-H…O and a C-H…π(arene) interaction per molecule and link columns into 2D sheets (similar to Fig. 2) and ultimately the 2D sheets are weakly linked into a 3D structure. The **NpmF** and **NpoF** structures are **isomorphous** and are **isostructural** at the primary hydrogen bonding level **(Figure 3 supplementary diagram below).** The C_5N/amide and C_6/amide angles in **NpoF** are 27.06(15)° and 51.39(12)°. We have noted this effect in two **isomorphous** difluoro-*N*-(3-pyridyl)benzamides previously in Acta Cryst. (2009). C**65**, o345–o351 where two compounds (**24m**, **25m**) are isomorphous but not isostructural and another pair (**34m**, **35m**) which are essentially isomorphous and quasisostructural. The latter *are interesting examples of two isomers with similar unit-cell parameters and gross packing but which display quite different intermolecular interactions at the primary level due to subtle packing differences at the atom/group/ring level arising from differences in the peripheral ring-substitution patterns*.

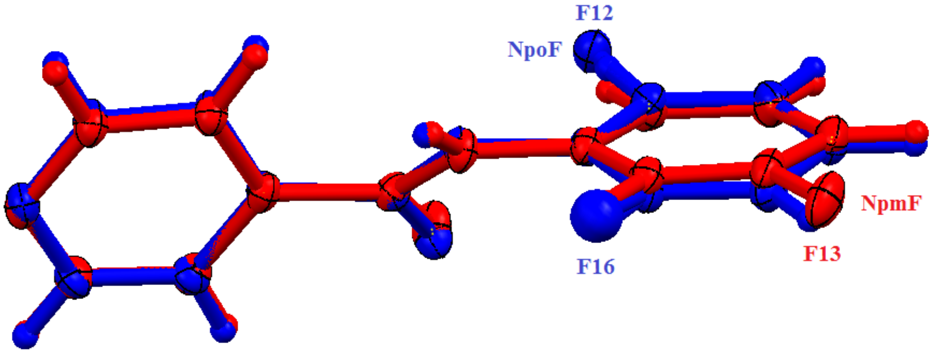

Figure 3 A molecular overlay of the isomorphous molecules of **NpmF** (in **red**) and **NpoF** (in **blue**) in space group *Cc* (using the Mercury package). The F-atom positional disorder in **NpoF** is depicted where the major component has the **F-***anti* conformation (as in **Figure 8**).

4.2 NmxF series of NmpF, NmmF and NmoF

The three **NmxF** compounds all aggregate *via* intermolecular N-H…$N_{pyridine}$ interactions. The **NmpF** crystal structure assembles as an unusual hydrogen bonded tetrameric unit linked by rather long N-H…N hydrogen bonds in addition to flanking but weaker intramolecular C-H…N interactions (from C$16_{[A-D]}$...N23 and C$22_{[A-D]}$...N23).

4.2.1 NmpF molecular and crystal structure [9-06] – 'The *St. Brigid's* cross'

The **NmpF** isomer crystallizes in the space group $P\bar{1}$ (No. 2) with *Z*' = 4, which is quite unusual and rather unexpected for this benzamide derivative. The four molecules (A) to (D) form a hydrogen bonded cyclic tetrameric assembly with four independent molecules within the asymmetric unit and *via* long N-H…$N_{pyridine}$ hydrogen bonds. There are distinct differences between the rather long $_{\mathbf{amide}}$**N1-H1…N23**$_{\mathbf{pyridine}}$ intermolecular distances of 3.171(2), 3.193(2), 3.224(2), 3.254(2) Å (a difference of 0.08 Å) with all of the N…N distances significantly different. In tandem with each of the four N-H…$N_{pyridine}$ interactions are two slightly longer and weaker flanking C-H…N_{pyr} interactions forming $R^1_2(6)$ and $R^1_2(7)$ rings with an overall size of $R^1_3(9)$. The molecules aggregate as four-membered molecular rings as [A→D→B→C→A] (**Figure 4**) to give a compact four molecule assembly as a hydrogen bonded $R^4_4(24)$ ring (considering the principal N-H...N interaction). The intermolecular range of the four **C22**$_{\mathbf{A-D}}$**…N23**$_{\mathbf{A-D}}$ distances are from 3.366(2) to 3.403(2) Å [and similar to **C16$_{A-D}$…N23$_{A-D}$**]. These are the only C-H…N interactions of significance in the **NmpF** tetramer assembly and subtle differences between the various interactions allow us to easily distinguish and note the differences between the four independent molecules (the **Nm** ring is **N-*syn***). The closest overlap of aromatic groups and π…π stacking is 3.40 Å. The C12$_{A-D}$…O1$_{A-D}$ contact is also present in the tetramer. Of interest is that the tetramers are further linked by C-H…F/O=C interactions. The four rather short C-H…F interactions are in the range for C…F distances of 3.266(2) to 3.281(2) Å and there are also some short C-H…O=C interactions present in the crystal structure linking the tetrameric assemblies.

Analysis of the centres of each of the four molecules in PLATON reveals that there are only similarities for the z axis components and no other relationships are present as revealed by (0.32, 0.96, 0.13), (0.24, 0.37, 0.13), (0.04, 0.76, 0.37), (0.63, 0.68, 0.37). It is possible that data collected over a range of different temperatures may reveal a phase transition but this possibility has not been explored (the RT [294 K] **NmpF** structure is similar to the LT data).

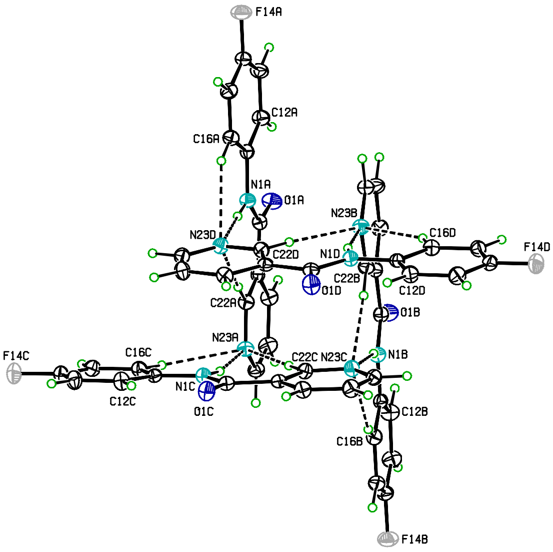

Figure 4 NmpF hydrogen bonded tetramer.

Crystallization with *Z'* = 4 is rather unusual but there are many cases available on the CSD, [495 examples with 3D coordinates and *R* < 0.1 in space group $P\bar{1}$ or 1705 'hits' for the entire CSD (version 4.29 + 3 updates)]. Molecules (A) to (D) differ slightly within the tetrameric assembly and without molecular disorder; importantly there are no matrix correlation coeffecients above 0.5. The N-H and pyridine N are oriented in the same direction and this facilitates either dimer or chain formation (catemer) at least. The transformation could be metrically to monoclinic but the unit cell data would be transformed from 9.759, 9.764, 21.170, 96.14°, 95.74°, 90° to 13.805, 13.804, 21.170, 89.71°, 98.41°, 90.03° which is NOT even close to being metrically monoclinic. Molecules A, C and B, D can be further paired as both of these pairs of molecules have similar geometric data. For example, the intramolecular C_6/C_5N interplanar angles are 5.42(9)°, 0.77(10)°, 5.39(9)°, 0.74(9)° for molecules (A) to (D) indicating that [A, C] and [B, D] can be paired. The **NmpF** structure could be the subject of further study to see if there is a temperature dependence on the crystal structure. The related benzamide **DIBCOH** is of interest but has N-H…O=C interactions.

4.2.2 NmmF molecular and crystal structure [9-16]

The **NmmF** crystal structure is regular with intermolecular N–H…N$_{\text{pyridine}}$ interactions as *C*(6) *zig-zag* helical chains and without disorder: the N1…N23 distance is longer than for **NpmF** above at 3.1146(18) Å (the flanking C-H…N with H…N23 = 2.67 Å is not significant). There is a significant C-H…O=C interaction and two weaker C-H…π(arene) interactions involving C15 and C22. The combination of N-H…N, C-H…O=C and two weaker interactions gives rise to a rumpled 2-D sheet parallel to the $(10\bar{1})$ plane. The angle between the C_6/C_5N planes is 50.16(5)°,whereas the C_5N/amide and C_6/amide are intermediate between this angle at 24.00(7)° and 27.47(5)°.

4.2.3 NmoF molecular and crystal structure [8-13]

The **NmoF** structure crystallizing in $P2_12_12_1$ is regular and without any problems. In **NmoF** the orientation of the pyridinyl N23 and fluoro F12 atoms are *cisoid* with respect to one another and *transoid* to the carbonyl oxygen atom O1 [**NmoF** has the **N-*syn*/F-*syn*** conformation]. In **NmoF** the C_5N and C_6 aromatic rings are mutually oriented at an angle of 22.67(14)°. Of further significance is that, in addition to the expected twisting, there is also some slight bending of the amide group with respect to the two terminal aromatic rings, with atom C11 by 0.139(11) Å and atom C21 by 0.009(13) Å from the three atom amide group (O/C/N) and positioned on the same side (to emphasize the overall bending), though the bending especially manifests at C11 and is presumably due to crystal packing forces. The {C11…C16} rings overlap slightly on stacking along the [100] direction with a close contact between C12...C15^i of 3.307(5) Å, and this is 0.10 Å less than the C atom radii sum {symmetry code *i* = 1+x,y,z}. In **NmoF** the amido N1-H1 forms an intramolecular N1-H1...F12 *ortho* contact: another contact C16-H16...O1 is also present. Intermolecular contacts manifest as N1-H1...N23* as the shortest (N1...N23* distance of 3.182(4) Å) generating a *zig-zag* one-dimensional helical chain along the *a*-axis direction as a stacked herringbone column (along the 2_1 symmetry axis) (**Figure 5**). The primary N1-H1…N23* interactions as *C*(6) chains (as in **NmmF** above) are augmented by a flanking

C22-H22…N23* (**Figure 5**) interaction forming $R^1_2(7)$ rings (however both the N…N/C…N distances in this ring are rather long, though symmetrical). Other weaker interactions involving C-H...N/O/F generate a 3D network, although these interactions are secondary and much weaker in nature.

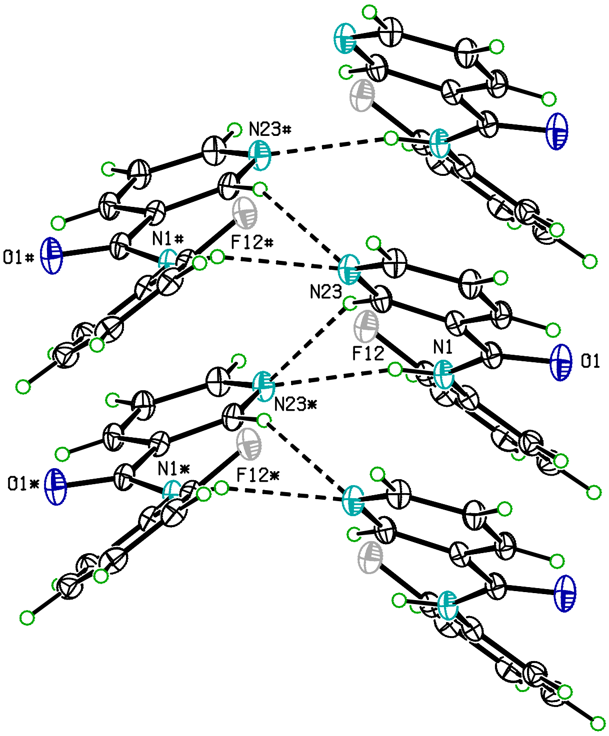

Figure 5 The N-H…N hydrogen bonding in **NmoF** aggregates as *zig-zag* helical chains along the *a*-axis direction together with C-H...N: molecules with labels # and * are positioned at the symmetry equivalent positions 1/2+x, -1/2-y, -z and -1/2+x, -1/2-y, -z, respectively.

4.3. NoxF series

The primary hydrogen bonding in all three **NoxF** derivatives is aggregation *via* N-H…$N_{pyridine}$ interactions but these are *intramolecular* interactions as $_{amide}$N-H…$N_{pyridine}$ for **NopF**, **NomF** and **NooF**. There is a clear lack of strong hydrogen bonding in these three **NoxF** systems apart from the intramolecular N-H…N_{pyr}. The **NopF** and **NooF** also contain a minor component of chlorine impurity (4%) in their respective crystal structures that arose in the original synthesis and proved difficult to separate by chromatography. Only the minor Cl atom site was included in the refinement.

4.3.1 NopF molecular and crystal structure [9-04]

The **NopF** structure crystallizes in $P2_1/c$ and refines to an R-factor of 7%. In the latter stages of refinement it was noticed that a minor peak was present in close proximity to H25 with a peak height of 0.55 e.Å^{-3}: the next highest peak was at 0.20 e.Å^{-3}. This atom site is situated at a distance of only 1.20 Å from the C25 atom. Refinement initially with a minor F atom site was finalised with a Cl atom to give site occupancy of *ca*. 4% [at 4.2(4)%]. This is the optimum site value although the apparent bond length is very short for a C-X and this can be attributed to many factors not least the fact that librational motion could be a issue. The minor C atom sites were not modelled accordingly as they are in such low occupancy that 4% C atoms are essentially merged with background ‘noise’. The chloro atom site is treated as if it were part of the principal molecule given that it is not practical to refine 4% of the C/N/O molecular backbone as a minor component. In **NopF** the angle between the C_6/C_5N planes is 30.34(10)° whereas the C_5N/amide are co-planar at 4.75(15)°. The structure is remarkable for the lack of strong hydrogen bonds and the only hydrogen bond of consequence is the intramolecular N1-H1…N22 hydrogen bond [N…N 2.679(3) Å] that enforces quasi-parallel alignment of the aromatic rings in tandem with an intramolecular C-H…O interaction. A C-H…O interaction further links the **NopF** molecules into 1D chains along the *b*-axis direction and weak C-H…F interactions link chains into sheets and complete the structure with molecules forming weak interactions along the *b*-axis direction and parallel to the $(10\,\bar{2})$ plane. On the CSD [paper reference 8], **GEPQIC** is the parent chloro derivative [as **NopCl**] instead of containing an F atom as for **NopF**. **WUVYIV** (Br) is isomorphous with the Cl derivative **GEPQIC** although this is not stated on the CSD. The molecular overlay between the Cl/Br analogues is within 0.005 Å and the angles between the C_6/C_5N rings close to 0°. The **NopF** structure has also been reported by Wilson and Munro, *Acta Cryst.* C, **66**, 2010, 513-516 while our manuscript was being reviewed (submitted **22nd June 2010**). Their **NopF** structure does not contain the chloro impurity and this is probably due to the different synthetic and crystallisation methods (see Page 36) employed by our respective groups.

4.3.2 NomF molecular and crystal structure [9-07]

The **NomF** structure contains two molecules (Z'=2) which are similar, in the asymmetric unit of space group $P2_1/n$. One of the molecules is disordered with a major *meta*-F atom site of 0.939(5) at F13A and the minor site at F15A with 0.061(5) unit site occupancy. The disorder is simple in that it only involves 180° rotation about the N1-C11 bond and there are no other unusual artefacts of disorder in the structure [no minor chloro site component was detected in the *meta*-position near C25A/B as for **NopF**]. The other differences between the two molecules are in the bond lengths and angles *e.g.* the C1-N1-C11-C16 torsion angle is 177.6(3)° in molecule (A) and 172.0(3)° in (B). Other differences between (A) and (B) are less significant. As for **NopF**, the **NomF** structure is remarkable for the lack of strong hydrogen bonds in that the strongest hydrogen bond is the intramolecular $N\text{-}H\ldots N_{pyridine}$ at 2.675(4) Å in (A) and 2.655(4) Å in (B). Two intramolecular C-H…O interactions are also noted involving C12A/B at 2.845(4) Å and 2.895(4) Å. Otherwise, there are no other direction specific interactions (**Figure 6**) apart from a C-H…O=C interaction that links (A) and (B) molecules within the asymmetric unit. The angles between the C_6/C_5N planes are 4.4(2)/4.6(2)° for molecules (A) and (B), whereas the C_5N/amide and C_6/amide are 2.0(2)/4.2(2)° and 5.5(2)/6.4(2)°.

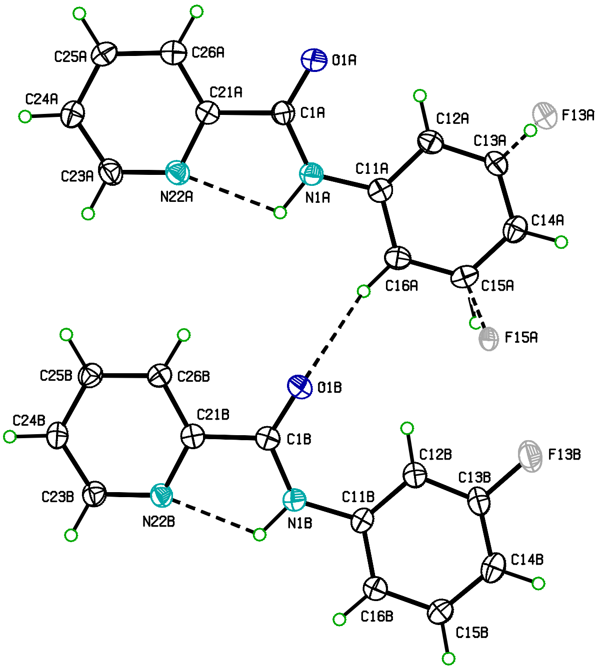

Figure 6 An ORTEP diagram of the two molecules (A) and (B) in the asymmetric unit of **NomF** with displacement ellipsoids drawn at the 30% probability level. The minor component of disorder in molecule (A) is shown at C15-H15 (as detailed in **Figure 8**).

4.3.3 NooF molecular and crystal structure [8-14]

In **NooF** the molecular structure (**Figure 7**) is essentially planar with only a small twisting (<10°) of the three principal groups from co-planarity. A minor impurity of a chloro atom is present in a *meta* position on the pyridinyl ring [at 3.2(3)%]. Only this minor Cl atom site was included in the refinement and the major/minor atom sites were assumed to be coincidental in the **NooF** molecular structure. As discussed for the **NopF** structure above, it is not practical to refine 3% occupancy for the minor backbone component; the structural results will not be improved by this additional refinement. As in **NmoF**, there is some slight bending of the amide group with respect to the two terminal aromatic rings, with C11 at 0.087(9) Å and C21 at 0.033(11) Å from the three atom O1/C1/N1 amide group and C11/C21 positioned on the same side. In **NooF** there are two distinct intramolecular interactions observed *via* the amido group as (*a*) N1-H1...F12 with the *ortho*-F12 atom {N1…F12 = 2.654(2) Å, N1-H1…F12 = 103°} and (*b*) N1-H1…N22 with the *ortho*-N22 atom {N1…N22 = 2.630(3) Å and N1-H1…N22 = 117(2)°}: another contact C16-H16...O1 is also noted. There are no intermolecular N1-H1…X interactions (X = C/N/O/F) in **NooF** with the closest C atom located at 3.539(3) Å distance (C16 at the symmetry equivalent position 1+x,y,z) and at 3.577(3) Å for C23 (located at x-1,y,z) from the amide N1. The closest H atom contact is H23 at 3.30 Å (at the symmetry position –x,-y,-z). The lack of H bonding involving N1-H1 is of interest as it is the strongest donor group in **NooF**. This effect derives from the presence of the two intramolecular N1-H1…F12 and N1-H1…N22 interactions and intermolecular steric packing effects which prevents the close approach of suitable of acceptor atoms/groups to interact with the N1-H1 donor group. The effect is also observed in the ^{1}H NMR in DMSO-d$_6$. A minor stacking contact is noted with C1…C23 (at x-1,y,z) at a distance of 3.337(3) Å which manifests along the *a*-axis direction. Overall **NooF** is of interest as it is a potentially useful ligand for coordination chemistry with an N/N/F donor set.

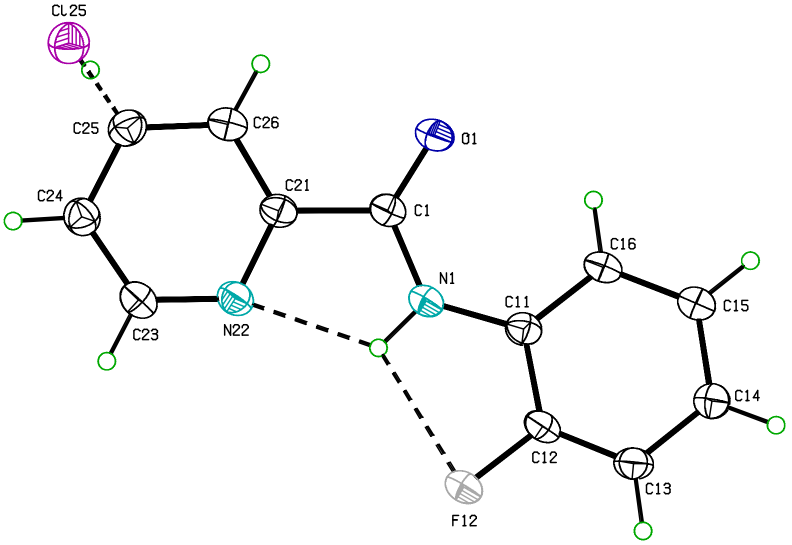

Figure 7 A view of the **NooF** molecule with intramolecular N-H…N/F interactions depicted as dashed lines: displacement ellipsoids are depicted at the 30% probability level.

4.4. Table 1. Experimental details for the nine NxxF isomers

Experiments were carried out with Mo $K\alpha$ radiation using a Nonius KappaCCD diffractometer. Absorption was corrected for by multi-scan methods, (*SORTAV*; Blessing, 1995). H atoms were treated by a mixture of independent and constrained refinement. For the three isomers **NpmF**, **NpoF** and **NmoF** the calculated Flack parameter from refinement is meaningless. **NopF** and **NooF** contain a minor Cl component that originated from the original synthesis.

	NppF-[9-08]	**NpmF**-[9-17]	**NpoF**-[9-09]	**NmpF**-[9-06]	**NmmF**-[9-16]
Crystal data					
Chemical formula	$C_{12}H_9FN_2O$	$C_{12}H_9FN_2O$	$C_{12}H_9FN_2O$	$C_{12}H_9FN_2O$	$C_{12}H_9FN_2O$
M_r	216.21	216.21	216.21	216.21	216.21
Crystal system, space group	Triclinic, $P\bar{1}$	Monoclinic, *Cc*	Monoclinic, *Cc*	Triclinic, $P\bar{1}$	Monoclinic, $P2_1/n$
Temperature (K)	200	150	150	150	150
a, *b*, *c* (Å)	5.4260(2), 7.4928(3), 24.0074(9)	11.0723(7), 12.8655(8), 7.9596(3)	10.9275(5), 12.8165(4), 8.2422(4)	9.7585(3), 9.7644(2), 21.1700(6)	8.8514(6), 12.1628(10), 9.6489(5)
α, β, γ (°)	80.9694(18), 90.041(2), 90.243(2)	90, 114.444(4), 90	90, 117.130(2), 90	96.1397(17), 95.7365(14), 89.9958(18)	90, 105.823(4), 90
V (Å^3)	963.94(6)	1032.22(10)	1027.33(8)	1995.47(9)	999.42(12)
Z	4	4	4	8	4
μ (mm^{-1})	0.11	0.10	0.10	0.11	0.11
Crystal size (mm)	0.25 × 0.10 × 0.08	0.36 × 0.16 × 0.16	0.32 × 0.30 × 0.26	0.32 × 0.26 × 0.18	0.30 × 0.16 × 0.15
Data collection					
T_{min}, T_{max}	0.973, 0.991	0.964, 0.984	0.968, 0.974	0.967, 0.981	0.969, 0.984
No. of measured, independent and observed reflections	4341, 4341, 3270 $\{I > 2\sigma(I)\}$	3643, 1176, 989 $\{I > 2\sigma(I)\}$	3196, 1165, 1013 $\{I > 2\sigma(I)\}$	22261, 8999, 6611 $\{I > 2\sigma(I)\}$	6578, 2271, 1595 $\{I > 2\sigma(I)\}$
R_{int}	0.00	0.078	0.041	0.049	0.034
Refinement					
$R[F^2 > 2\sigma(F^2)]$, $wR(F^2)$, S	0.051, 0.142, 1.03	0.042, 0.113, 1.04	0.051, 0.135, 1.06	0.050, 0.124, 1.04	0.044, 0.118, 1.05
No. of reflections	4341	1176	1165	8999	2271
No. of parameters	299	150	154	593	150
No. of restraints	0	2	3	0	0
$\Delta\rangle_{max}$, $\Delta\rangle_{min}$ (e Å^{-3})	0.23, -0.23	0.18, -0.25	0.22, -0.24	0.23, -0.24	0.22, -0.25

	NmoF-[8-13]	**NopF**-[9-04]	**NomF**-[9-07]	**NooF**-[8-14]
Crystal data				
Chemical formula	$C_{12}H_9FN_2O$	$C_{12}H_{8.96}Cl_{0.04}FN_2O$	$C_{12}H_9FN_2O$	$C_{12}H_{8.97}Cl_{0.03}FN_2O$
M_r	216.21	217.68	216.21	217.33
Crystal system, space group	Orthorhombic, $P2_12_12_1$	Monoclinic, $P2_1/c$	Monoclinic, $P2_1/n$	Monoclinic, $P2_1/n$
Temperature (K)	150	150	150	150
a, b, c (Å)	4.0813(2), 10.7319(7), 22.5900(11)	8.0622(9), 6.0665(4), 20.392(2)	5.7289(2), 23.2077(13), 15.1001(9)	4.8030(4), 19.1318(18), 10.8759(8)
α, β, γ (°)	90, 90, 90	90, 95.296(4), 90	90, 95.260(3), 90	90, 99.276(5), 90
V (Å^3)	989.44(9)	993.10(16)	1999.17(18)	986.32(14)
Z	4	4	8	4
μ (mm^{-1})	0.11	0.12	0.11	0.12
Crystal size (mm)	0.12 × 0.08 × 0.08	0.34 × 0.20 × 0.03	0.26 × 0.16 × 0.14	0.20 × 0.15 × 0.03
Data collection				
T_{min}, T_{max}	0.987, 0.991	0.961, 0.996	0.973, 0.985	0.979, 0.997
No. of measured, independent and observed reflections	4223, 1364, 957 $\{I > 2\sigma(I)\}$	6521, 2234, 1187 $\{I > 2\sigma(I)\}$	13916, 4454, 2033 $\{I > 2\sigma(I)\}$	6707, 2238, 1160 $\{I > 2\sigma(I)\}$
R_{int}	0.051	0.101	0.073	0.077
Refinement				
$R[F^2 > 2\sigma(F^2)]$, $wR(F^2)$, S	0.049, 0.125, 1.04	0.063, 0.166, 1.03	0.074, 0.223, 1.07	0.057, 0.154, 1.00
No. of reflections	1364	2234	4454	2238
No. of parameters	149	154	307	154
No. of restraints	0	0	0	0
$\Delta\rangle_{max}$, $\Delta\rangle_{min}$ (e Å^{-3})	0.25, -0.23	0.19, -0.24	0.36, -0.30	0.22, -0.21

Computer programs: *KappaCCD Server Software* (Nonius, 1997), *DENZO-SMN* (Otwinowski and Minor, 1997), *SHELXS97* (Sheldrick, 2008), *SHELXL97* (Sheldrick, 2008) and SORTX (McArdle, 1995), *PLATON* (Spek, 2003), *PLATON* (Spek, 2009), *SHELXL97* and PREP8 (Ferguson, 1998).

4.5 **Table 2. Selected hydrogen-bond parameters for the nine NxxF isomers.**

D—H···*A*	*D*—H (Å)	H···*A* (Å)	*D*···*A* (Å)	*D*—H···*A* (°)
NppF-[9-08]				
N1A—H1A···O1A[i]	0.88 (3)	2.42 (3)	3.203 (2)	150 (2)
N1B—H1B···O1B[ii]	0.82 (3)	2.46 (3)	3.216 (2)	154 (2)
C12A—H12A···O1A	0.95	2.40	2.900 (3)	113
C12B—H12B···O1B	0.95	2.43	2.912 (3)	111
C16A—H16A···O1A[i]	0.95	2.58	3.280 (2)	131
C16B—H16B···O1B[ii]	0.95	2.55	3.275 (3)	133
NpmF-[9-17]				
N1—H1···N24[iii]	0.88 (4)	2.12 (4)	2.991 (4)	169 (4)
C15—H15···O1[iv]	0.95	2.56	3.202 (4)	125
C16—H16···O1	0.95	2.54	2.946 (4)	106
C25—H25···Cg1[v]	0.95	2.65	3.484 (3)	147
NpoF-[9-09]				
N1—H1···N24[iii]	0.92 (5)	2.02 (5)	2.930 (4)	169 (4)
C13—H13···O1[iv]	0.95	2.56	3.162 (4)	122
C26—H26···O1[vi]	0.95	2.54	3.291 (4)	136
C25—H25···Cg1[v]	0.95	2.70	3.564 (4)	151
NmpF-[9-06]				
N1A—H1A···N23D	0.854 (19)	2.359 (19)	3.193 (2)	165.2 (16)
N1B—H1B···N23C	0.827 (19)	2.42 (2)	3.224 (2)	165.2 (18)
N1C—H1C···N23A	0.865 (18)	2.329 (19)	3.171 (2)	164.4 (15)
N1D—H1D···N23B	0.826 (19)	2.449 (19)	3.254 (2)	165.1 (16)
C16A—H16A···N23D	0.95	2.53	3.368 (2)	148
C16B—H16B···N23C	0.95	2.53	3.379 (2)	150
C16C—H16C···N23A	0.95	2.52	3.364 (2)	147
C16D—H16D···N23B	0.95	2.53	3.387 (2)	150
C22A—H22A···N23D	0.95	2.44	3.387 (2)	178
C22B—H22B···N23C	0.95	2.43	3.380 (2)	177
C22C—H22C···N23A	0.95	2.42	3.366 (2)	177
C22D—H22D···N23B	0.95	2.45	3.403 (2)	176
C12A—H12A···O1A	0.95	2.23	2.842 (2)	122
C12B—H12B···O1B	0.95	2.24	2.853 (2)	121
C12C—H12C···O1C	0.95	2.23	2.840 (2)	122
C12D—H12D···O1D	0.95	2.24	2.858 (2)	122
NmmF-[9-16]				
N1—H1···N23[vii]	0.896 (18)	2.253 (19)	3.1146 (18)	161.3 (16)
C12—H12···O1	0.95	2.38	2.8959 (19)	114
C14—H14···O1[viii]	0.95	2.39	3.2375 (19)	149

C15—H15···Cg1$^{\text{ix}}$	0.95	2.82	3.5574 (17)	135
C22—H22···Cg2$^{\text{x}}$	0.95	2.77	3.4486 (18)	129
NmoF-[8-13]				
N1—H1···N23$^{\text{xi}}$	0.87 (3)	2.33 (3)	3.182 (4)	166 (4)
N1—H1···F12	0.87 (3)	2.37 (3)	2.686 (3)	102 (2)
C16—H16···O1	0.95	2.47	2.909 (4)	108
C13—H13···O1$^{\text{xii}}$	0.95	2.54	3.345 (4)	143
C22—H22···N23$^{\text{xi}}$	0.95	2.52	3.348 (4)	147
C24—H24···F12$^{\text{xiii}}$	0.95	2.37	3.059 (4)	129
C25—H25···O1$^{\text{xiv}}$	0.95	2.56	3.458 (4)	158
NopF-[9-04]				
N1—H1···N22	0.90 (3)	2.20 (3)	2.679 (3)	113 (2)
C12—H12···O1	0.95	2.40	2.925 (3)	115
C16—H16···O1$^{\text{xv}}$	0.95	2.36	3.238 (3)	154
C25—H25···F14$^{\text{xvi}}$	0.95	2.55	3.408 (3)	150
NomF-[9-07]				
N1A—H1A···N22A	1.00 (3)	2.20 (3)	2.675 (4)	108 (2)
N1B—H1B···N22B	0.98 (3)	2.11 (3)	2.655 (4)	113 (2)
C12A—H12A···O1A	0.95	2.23	2.845 (4)	122
C12B—H12B···O1B	0.95	2.29	2.895 (4)	121
C16A—H16A···O1B	0.95	2.49	3.362 (4)	152
NooF-[8-14]				
N1—H1···F12	0.92 (2)	2.29 (2)	2.654 (2)	102.8 (16)
N1—H1···N22	0.92 (2)	2.09 (2)	2.630 (3)	116.2 (17)
C14—H14···O1$^{\text{iv}}$	0.95	2.55	3.298 (3)	136
C16—H16···O1	0.95	2.37	2.950 (3)	119

Symmetry code(s): (i) *x*+1, *y*, *z*; (ii) *x*-1, *y*, *z*; (iii) *x*-1/2, -*y*-1/2, *z*-1/2; (iv) *x*-1/2, -*y*+1/2, *z*-1/2; (v) *x*+1/2, *y*-1/2, *z*; (vi) *x*, -*y*, *z*-1/2; (vii) *x*+1/2, -*y*+1/2, *z*+1/2; (viii) *x*+1/2, -*y*+3/2, *z*+1/2; (ix) -*x*+1/2, *y*+1/2, -*z*+3/2; (x) -*x*, -*y*+1, -*z*+1; (xi) *x*-1/2, -*y*-1/2, -*z*; (xii) -*x*, *y*-1/2, -*z*+1/2; (xiii) *x*+1/2, -*y*-1/2, -*z*; (xiv) *x*+1/2, -*y*+1/2, -*z*; (xv) *x*, *y*+1, *z*; (xvi) *x*-1, -*y*-1/2, *z*-1/2.

5. *Ab initio* calculation results

5.1. Energy results

5.1.1. Table 3. Optimisations in *gas phase*

	E_{SCF}	δE_{SCF}	E_0	δE_0	E	δE	G	δG
NppF	-743.1027	0.00	-746.0984	0.00	-746.0856	0.00	-746.1394	0.00
NpmF	-743.1048	-5.43	-746.0991	-1.73	-746.0863	-1.78	-746.1401	-1.68
NpoF	-743.1041	-3.50	-746.0998	-3.66	-746.0871	-3.80	-746.1406	-3.13
NmpF	-743.1051	-6.08	-746.0992	-2.16	-746.0865	-2.13	-746.1403	-2.30
NmmF	-743.1072	-11.79	-746.0999	-3.99	-746.0872	-4.04	-746.1409	-3.86
NmoF	-743.1063	-9.36	-746.1004	-5.29	-746.0877	-5.38	-746.1413	-4.91
NopF	-743.1145	-30.99	-746.1096	-29.50	-746.0970	-29.95	-746.1502	-28.26
NomF	-743.1168	-36.84	-746.1104	-31.52	-746.0979	-32.07	-746.1508	-29.83
NooF	-743.1148	-31.66	-746.1098	-29.88	-746.0972	-30.43	-746.1501	-28.11

5.1.2. Table 4. Optimisations in CH_2Cl_2

	E_{SCF}	δE_{SCF}	E_0	δE_0	E	δE	G	δG
NppF	-743.1297	-4.62	-746.12261	-3.10	-746.1100	-3.18	-746.1632	-3.17
NpmF	-743.1317	-9.80	-746.12326	-4.83	-746.1106	-4.89	-746.1639	-5.12
NpoF	-743.1280	0.00	-746.12142	0.00	-746.1088	0.00	-746.1620	0.00
NmpF	-743.1319	-10.40	-746.12295	-4.01	-746.1103	-4.07	-746.1635	-4.02
NmmF	-743.1340	-15.81	-746.12368	-5.93	-746.1110	-5.96	-746.1644	-6.31
NmoF	-743.1302	-5.98	-746.12174	-0.84	-746.1091	-0.80	-746.1623	-1.02
NopF	-743.1372	-24.36	-746.13020	-23.03	-746.1176	-23.21	-746.1706	-22.73
NomF	-743.1393	-29.68	-746.13107	-25.34	-746.1184	-25.43	-746.1718	-25.82
NooF	-743.1355	-19.69	-746.12858	-18.79	-746.1160	-19.14	-746.1687	-17.57

5.1.3. Table 5. Optimisations in H_2O

	E_{SCF}	δE_{SCF}	E_0	δE_0	E	δE	G	δG
NppF	-743.1245	-7.25	-746.11620	-6.78	-746.1043	-8.83	-746.1555	-3.73
NpmF	-743.1262	-11.79	-746.11632	-7.12	-746.1037	-7.07	-746.1571	-7.78
NpoF	-743.1217	0.00	-746.11361	0.00	-746.1010	0.00	-746.1541	0.00
NmpF	-743.1269	-13.46	-746.11635	-7.20	-746.1036	-6.84	-746.1562	-5.39
NmmF	-743.1288	-18.61	-746.11666	-8.01	-746.1040	-8.03	-746.1572	-8.08
NmoF	-743.1243	-6.88	-746.11406	-1.17	-746.1014	-1.03	-746.1549	-1.97
NopF	-743.1294	-20.22	-746.12095	-19.26	-746.1091	-21.37	-746.1603	-16.11
NomF	-743.1313	-25.20	-746.12198	-21.96	-746.1101	-23.89	-746.1615	-19.49
NooF	-743.1271	-14.22	-746.11920	-14.68	-746.1065	-14.59	-746.1600	-15.57

The Tables present absolute values of electronic (E_{SCF}), zero point (E_0), energy (E) and Gibbs free energy (G) for the nine **NxxF** isomers expressed in Hartrees (E_h). The relative energies (**NppF** or **NpoF** is taken as basis point) are shown in columns with suffix δ, and are expressed in $kJ.mol^{-1}$.

5.1.4. Table 6. Comparison of energies in different media

	gas phase vs. CH_2Cl_2				*gas phase vs.* H_2O				CH_2Cl_2 *vs* H_2O				$logK_{D/W}$
	ΔE_{SCF}	ΔE_0	ΔE	ΔG_{solv}	ΔE_{SCF}	ΔE_0	ΔE	ΔG_{solv}	$\Delta\Delta E_{SCF}$	$\Delta\Delta E_0$	$\Delta\Delta E$	$\Delta\Delta G_{solv}$	
NppF	-70.81	-63.52	-63.87	-62.30	-57.08	-46.69	-49.09	-42.27	-13.73	-16.83	-14.79	-20.03	3.5089173
NpmF	-70.56	-63.51	-63.80	-62.57	-56.19	-45.29	-45.54	-44.64	-14.37	-18.21	-18.26	-17.93	3.1414697
NpoF	-62.69	-56.75	-56.89	-56.00	-46.33	-36.24	-36.46	-35.40	-16.35	-20.51	-20.43	-20.59	3.6073326
NmpF	-70.50	-62.26	-62.63	-60.86	-57.21	-44.94	-44.96	-41.63	-13.29	-17.32	-17.67	-19.23	3.3681927
NmmF	-70.21	-62.35	-62.61	-61.59	-56.66	-43.92	-44.24	-42.76	-13.55	-18.43	-18.36	-18.83	3.2987502
NmoF	-62.80	-55.97	-56.10	-55.24	-47.35	-35.79	-35.90	-35.60	-15.45	-20.18	-20.20	-19.64	3.4408544
NopF	-59.56	-53.95	-53.95	-53.61	-39.06	-29.67	-31.68	-26.39	-20.50	-24.28	-22.28	-27.22	4.7671608
NomF	-59.03	-54.23	-54.04	-55.13	-38.19	-30.34	-32.08	-28.20	-20.84	-23.89	-21.97	-26.93	4.7165735
NooF	-54.22	-49.33	-49.39	-48.59	-32.39	-24.71	-24.41	-26.00	-21.83	-24.62	-24.98	-22.60	3.9577644

The **Table 6** above shows differences (Δ) of the energies (E_{SCF}, E_0, E and G) for the nine **NxxF** isomers in different media expressed in $kJ.mol^{-1}$. The ΔG_{solv} represents the calculated energy of solvation, while $\Delta\Delta G_{solv}$ represents the difference of energies of solvation in two different solvents (CH_2Cl_2 and H_2O). The final variable, $logK_{D/W}$ presents the tentative (theoretical) values of the partition coefficient of the **NxxF** molecules between dichloromethane (CH_2Cl_2, DCM) and water (H_2O), calculated as $logK_{D/W} = - \Delta\Delta G_{solv}/2.303RT$. This model has not been validated using the exact experimental values of $logK_{D/W}$, therefore, it has exclusively relative (qualitative) not absolute (quantitative) significance and the tentative values of $logK_{D/W}$ should not be taken as final.

The energy calculation results (CBS-QB3) (Tables 3, 4, 5 and 6) comprise the electronic energies (δE_{SCF}) and Gibbs free energies (δG) in all three media, including ΔG_{solv} for CH_2Cl_2 and H_2O, as well as $\Delta\Delta G_{solv}$ (CH_2Cl_2 *vs.* H_2O). Differences between each molecule are given as δE_{SCF} (δG) and differences between media as ΔE_{SCF} (ΔG). The **NppF** energies are the *gas phase* reference points (least stable isomer) and **NpoF** energies for the solvents (as least stable). The large energy decrease for the **NoxF** triad is due to the intramolecular N1-H1…N22 interaction thus stabilising the **NoxF** molecular series. In addition, a weak stabilisation effect of the *meta*-F atom is discernible and these two effects make **NmoF** the most stable of the **NxxF** isomer grid.

The solvation of the **NxxF** isomers in CH_2Cl_2 is stabilizing and favourable, much more than solvation in H_2O. Differences in stabilisation among the nine isomers are considerable (Table 6). From **NppF** to **NooF** the stability gain (on solvation) decreases consistently. This solvation effect is greatest in the six **NpxF**, **NmxF** isomers compared to the **NoxF** triad which gain less stabilisation (in terms of energy decrease). The calculated $\Delta\Delta G_{solv}$ for CH_2Cl_2/H_2O (D/W) system are strongly positive, illustrating insolublity in H_2O (provisional $logK_{D/W}$ values based on $\Delta\Delta G_{solv}$ are 3-5). The **NoxF** triad should be the least soluble in H_2O ($\sim logK_{D/W}$ = 4-5); empirical observations confirm these calculated predictions.

5.2. Potential energy surface (PES) scans of the nine **NxxF** conformers (rotamers), optimised in *gas phase*

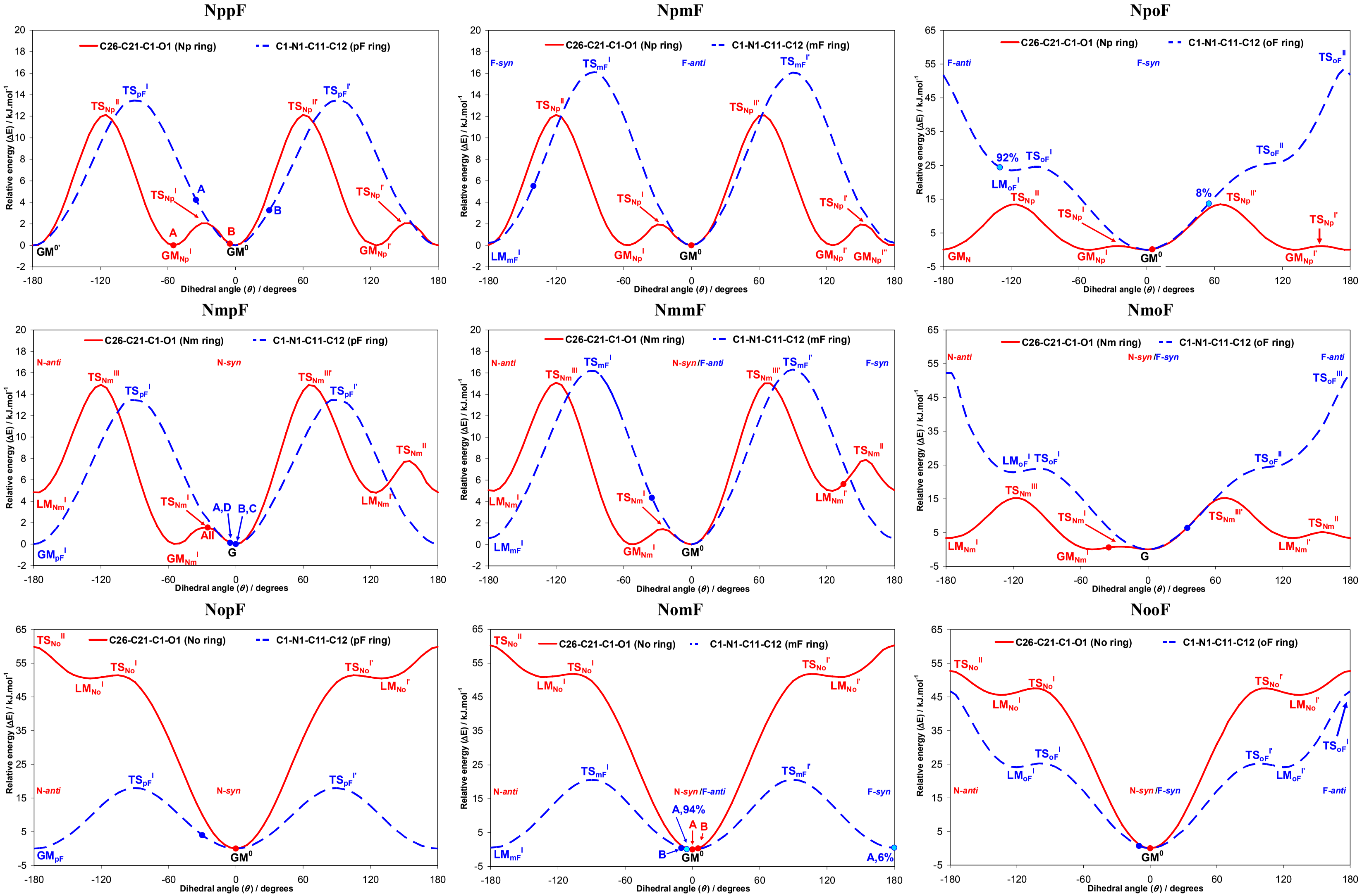

Detailed description:

The *para*-pyridine (**Np**) ring gives a PES profile with two global maxima located at *ca.* 60°, -120° (TS_{Np}^{II} = 12.01-13.43 kJ.mol^{-1}), two local maxima near -25°, 155° (TS_{Np}^{I} = 1.08-2.05 kJ.mol^{-1}). The four global minima are located at or near 0°, 125°, ±180° and -55°.

The *meta*-pyridine (**Nm**) ring gives a PES profile with two global minima *ca.* -50°, 0°, two global maxima near 65°, -120° (TS_{Nm}^{III} = 15.04±0.15 kJ.mol^{-1}) and two local minima *ca.* 125°, ±180° (LM_{Nm}^{I} = 3.33-5.00 kJ.mol^{-1}). The two local maxima are located at -25° (TS_{Np}^{I} = 0.83-1.55 kJ.mol^{-1}) and 155° (TS_{Np}^{II} = 5.15-7.90 kJ.mol^{-1}).

The *ortho*-pyridine (**No**) ring has a symmetrical PES profile with one global maximum at ±180° (TS_{No}^{II} = 52.70-60.24 kJ.mol^{-1}), two local maxima at ±105° (TS_{No}^{II} = 47.55-51.84 kJ.mol^{-1}), two local minima at ±135° (LM_{No}^{II} = 45.57-50.91 kJ.mol^{-1}) and one global minimum.

The *para*-fluorophenyl (**pF**) ring gives a PES profile with two global maxima at ±90° (TS_{pF}^{I} = 13.46-17.94 J.mol^{-1}) and two global minima at 0°, ±180°. The *meta*-fluorophenyl (**mF**) ring shows a PES profile with two global maxima near ±90° (TS_{mF}^{I} = 16.12-20.58 kJ.mol^{-1}), one local minimum at ±180° (LM_{mF}^{I} = 0.23-0.58 kJ.mol^{-1}) and one global minimum.

The *ortho*-fluorophenyl (**oF**) ring gives an asymmetrical PES profile in **NpoF** and **NmoF**, but symmetrical for **NooF**. There is a global maximum at ±180° (TS_{oF}^{II} = 46.69-52.17 kJ.mol^{-1}). **NpoF** and **NmoF** have one local maximum at -95° (TS_{oF}^{I} = 24.22±0.53 kJ.mol^{-1}), one local minimum at -120° (LM_{oF}^{II} = 23.17±0.48 kJ.mol^{-1}) and of note, a point of inflexion at 110° (TS_{oF}^{II} = 25.68±0.15 kJ.mol^{-1}). However, the symmetrical **NooF** has two local minima near ±120° (LM_{oF}^{I} = 24.09 kJ.mol^{-1}) and two local maxima at ±100° (TS_{oF}^{I} = 25.23 kJ.mol^{-1}).

Note on the NopF derivative:

The **NopF** structure has also been reported by C.R. Wilson and O.Q. Munro, *Acta Crystallographica* Section C, **66**, 2010, 513-516 [received from these authors by the IUCr Chester office on the **24th August 2010** and online **17th September 2010**] while our manuscript was under review (manuscript submitted to *CrystEngComm* on **22nd June 2010**). Their **NopF** structure does not contain a minor chloro component impurity in the crystal structure as it was made by a different route using the acid and amine in pyridine and with triphenylphosphite [by the method of Barnes *et al.*, *J. Chem. Eng. Data*, 1978, **23**, 349-350] and recrystallised subsequently from the solvent chloroform. Their reported **NopF** structure was also studied by Gaussian03 Revision C.02 at the B3LYP/6-31G** level and their structural and computational results are comparable to and analogous with our **NopF** results though no attempt was made to perform conformational analysis scans.

5.3. The PES conformational analysis diagrams for the nine **NxxF** isomers optimised in *gas phase* (full line), CH_2Cl_2 (dashed line) and in H_2O (dotted line)

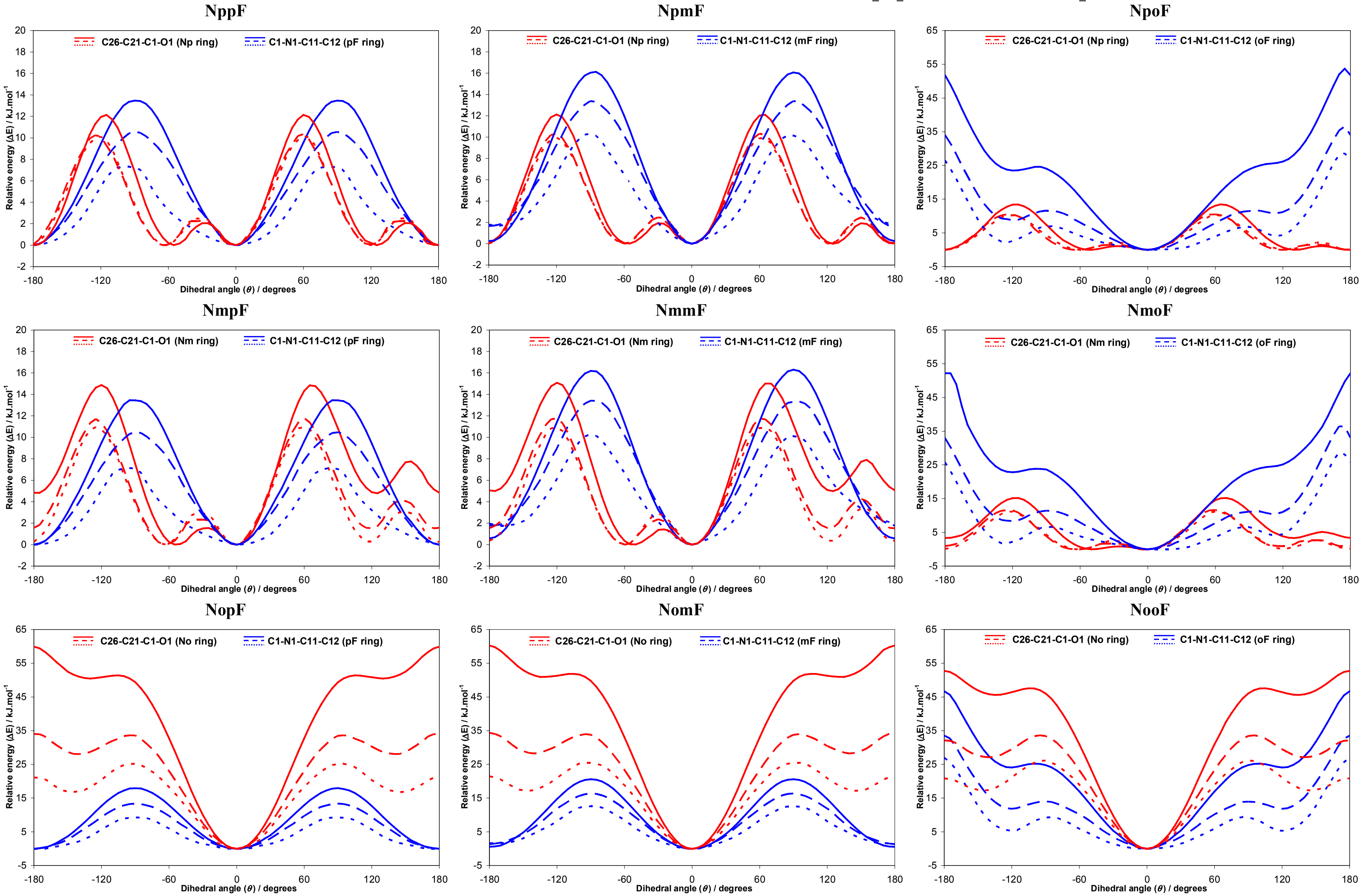

Description:
Rotational barriers (for conformational analysis under PCM-SMD solation model) decrease almost linear for the **pF** (~23% in CH_2Cl_2, ~59% in H_2O), **mF** (~19% in CH_2Cl_2, ~43% in H_2O) and **oF** rings (by ~46% in CH_2Cl_2, ~70% in H_2O) when compared with *gas phase* rotational barriers. There is a dramatic decrease for the **oF** ring with a change in the overall curve shape. For **Np** (~27%) and **Nm** (~28%) the decrease is similar for both solvents and for the **No** ring the rotational barrier drops by ~36% in CH_2Cl_2 and ~52% in H_2O. Another effect is the additional linear drops of LM_{Nm}^{I} and TS_{Nm}^{II} (by ~28% in CH_2Cl_2, ~45% in H_2O) and elevation of LM_{mF}^{I} (by an average of 1.24±0.27 $kJ.mol^{-1}$ in both solvents) and a shift of some of the minima in the **Np** and **Nm** rings by ±10°.